Modelling the impact of non-pharmaceutical interventions on workplace transmission of SARS-CoV-2 in the home-delivery sector

Carl A. Whitfield,[1,2,3] Martie van Tongeren,[4,3] Yang Han,[1] Hua Wei,[4,3] Sarah Daniels,[4,3] Martyn Regan,[5,4,3] David W. Denning,[2,3] Arpana Verma,[4,3] Lorenzo Pellis,[1] University of Manchester COVID-19 Modelling Group,[1] and Ian Hall[1,6,3]

[1]*Department of Mathematics, University of Manchester, Manchester, England*
[2]*Division of Infection, Immunity & Respiratory Medicine, School of Biological Sciences, University of Manchester, Manchester, England*
[3]*Manchester Academic Health Science Centre, University of Manchester, Manchester, England*
[4]*Division of Population Health, Health Services Research & Primary Care, School of Health Sciences, University of Manchester, Manchester, England*
[5]*National COVID-19 Response Centre, UK Health Security Agency, London, England*
[6]*Public Health, Advice, Guidance and Expertise, UK Health Security Agency, London, England*

Abstract

Objective: We aimed to use mathematical models of SARS-COV-2 to assess the potential efficacy of non-pharmaceutical interventions on transmission in the parcel delivery and logistics sector.

Methods: We developed a network-based model of workplace contacts based on data and consultations from companies in the parcel delivery and logistics sectors. We used these in stochastic simulations of disease transmission to predict the probability of workplace outbreaks in this settings. Individuals in the model have different viral load trajectories based on SARS-CoV-2 in-host dynamics, which couple to their infectiousness and test positive probability over time, in order to determine the impact of testing and isolation measures.

Results: The baseline model (without any interventions) showed different workplace infection rates for staff in different job roles. Based on our assumptions of contact patterns in the parcel delivery work setting we found that when a delivery driver was the index case, on average they infect only 0.18 other employees , while for warehouse and office workers this went up to 0.93 and 2.58 respectively. In the large-item delivery setting this was predicted to be 0.83, 0.94, and 1.61 respectively. Nonetheless, the vast majority of simulations resulted in 0 secondary cases among customers (even without contact-free delivery). Our results showed that a combination of social distancing, office staff working from home, and fixed driver pairings (all interventions carried out by the companies we consulted) reduce the risk of workplace outbreaks by 3-4 times.

Conclusion: This work suggests that, without interventions, significant transmission could occur in these workplaces, but that these pose minimal risk to customers. We found that identifying and isolating regular close-contacts of infectious individuals (i.e. house-share, carpools, or delivery pairs) is an efficient measure for stopping workplace outbreaks. Regular testing can make these isolation measures even more effective but also increases the number of staff isolating at one time. It is therefore more efficient to combine these measures with social distancing and contact reduction interventions, as these reduce both transmission and the number of people needing to isolate.

IMPORTANCE

During the COVID-19 pandemic the home-delivery sector has been vital to maintaining people's access to certain goods, and sustaining levels of economic activity for a variety of businesses. However, this important work necessarily involves contact with a large number of customers as well as colleagues. This means that questions have often been raised about whether enough is being done to keep customers and staff safe. Estimating the potential

risk to customers and staff is complex, but here we tackle this problem by building a model of workplace and customer contacts, from which we simulate SARS-CoV-2 transmission. By involving industry representatives in the development of this model, we have simulated interventions that have either been applied or considered, and so the findings of this study are extremely relevant to decisions made in that sector moving forward. Furthermore, we can learn generic lessons from this specific case study which apply to many types of shared workplace as well as highlighting implications of the highly stochastic nature of disease transmission in small populations.

I. INTRODUCTION

Demand for home-delivery services has spiked globally during the COVID-19 pandemic, as people have stayed at home to reduce transmission [1]. In the UK, non-essential retail shops were closed for much of 2020 and 2021, increasing the demand for online retail and home delivery. Additionally, stay-at-home orders brought new demand for large items such as furniture and white goods as many people adjusted to spending more time at home [2]. This new and displaced demand has, on the whole, been successfully absorbed and managed by the delivery and logistics sector, due in no small part to the efforts of the key workers in those sectors to keep business moving, while adapting to a changing work environment. Meanwhile, key workers in all sectors were disproportionately exposed to transmission of SARS-CoV-2 [3]. In the delivery sector, drivers and warehouse workers were also at risk, given their exposure to a large number of contacts, the likelihood of asymptomatic transmission in SARS-CoV-2, and the potential economic impact of absence due to the prevalence of flexible or zero-hours contracts in this sector. Furthermore, studies from other countries indicate that delivery drivers there could be at much greater risk [4, 5] than the general population, and so is a sector that requires greater attention.

Mathematical models have been central to understanding transmission of SARS-CoV-2 and in predicting the impact of various interventions. As more data has become available, models have been developed for a number of specific settings, including schools, hospitals, prisons and workplaces [6–9], to take into account the nuances and unique features of each setting. In this paper we present a model of delivery sector that has been uses to assess the impact of various measures that some companies have taken, as well as measures that were under consideration. One unique feature of these settings is the high number of brief contacts that delivery drivers have with members of the public, who themselves may otherwise have

very limited contacts. Another feature in the delivery of heavy or large items is the safety requirement for employees to handle and deliver goods in pairs, often requiring prolonged close contact and entry into customers' properties. Finally, there is still the poorly understood route of fomite transmission that has the potential to be important in this setting, due to the large volume of packages being handled. The model we present considers all of these aspects, and where data is unavailable or uncertain (e.g. for risk of fomite transmission), we consider a wide range of possible scenarios.

We have developed an agent-based network model with stochastic transmission. Therefore, each realisation of the simulation represents a possible chain of transmission within a workplace, and so conclusions can only be drawn from the aggregated results of many simulations. There are commonalities with several models in the literature, including the network models for COVID-19 transmission in workplaces [10]. The stochastic infection and isolation model is similar to other agent-based and branching process models [8, 11]. The model was developed based on a combination of epidemiological data and data and qualitative information gained from consultations with companies in the logistics sector in the UK.

As vaccines are rolled out globally, we expect the most severe impacts of COVID-19 on public health to be curtailed. However, containing the spread of new variants is likely to require good surveillance testing. There has been considerable debate around the usefulness of Lateral Flow Device (LFD) tests that can be self-administered and give rapid results [12–14]. Primarily, this centres around the lower sensitivity of LFD against Polymerase Chain Reaction testing (PCR), particularly at low viral loads [15], and the potential impact of false positives. However, recent data suggests that LFD specificity may be at least 99.9% [16], suggesting that false positives will have a negligible impact. Furthermore, culturable SARS-CoV-2 virus is only found, at most, in the first 8-10 days following symptom onset [17–19], when viral load is higher. This suggests that lower sensitivity tests may still be useful at detecting people when they are most infectious. However, the way tests are performed (e.g. self-administered vs. trained tester) can have an impact on sensitivity [20], plus the method of rollout (e.g. supervised vs. unsupervised testing) can affect the adherence to the testing policy. The model we present accounts for these various factors.

The aim of this paper is to estimate the efficacy of different workplace interventions with a model particularly tailored to the home-delivery sector. We considered several interventions and scenarios based on formal consultations with company representative from this sector. A secondary aim is to estimate the potential impact of presenteeism (working while sick)

with COVID-19 symptoms. Flexible or 'gig' contracts are common in the home delivery sector, as well as the use of self-employed couriers, all of which are factors associated with increased presenteeism [21], so this is an important factor to consider.

II. METHODS

A. Data Collection and Company Consultations

We carried out recorded consultations via teleconference with representatives from six companies between July and August 2020 (Round 1), and May and June 2021 (Round 2), three of these companies were interviewed in both rounds. Each semi-structured interview lasted 60-90 mins and was based around a set of open-ended questions regarding how the pandemic had impacted on the operations of the business and what measures had been put in place to protect staff and customers. As part of these consultations we asked questions regarding the number of staff working at typical sites and the frequency of contacts between employees and the public. Additionally, two companies provided data on staff numbers and deliveries, which are detailed in Appendix A 1. A summary report was sent to each company for comments and corrections to verify that we had interpreted their answers accurately, and the data correctly. Further details on the consultations are published in [2].

We also used data from an online contact survey aimed at delivery drivers in the UK [article in preparation], which received 170 responses (104 of which were from the workers involved in the delivery of small packages and/or large items). This survey was elective so was not statistically representative. The results of this survey are to be published elsewhere but a few results are utilised in this paper. Namely, only 5.3% reported working while having symptoms of COVID-19 or with a member of their household having a suspected or confirmed case of COVID-19. Conversely, 17.2% reported having isolated with symptoms of COVID-19 or due to a member of their household having a suspected or confirmed case of COVID-19. This suggests approximately 1 in 4 failing to isolate for one of these reasons. For this reason we consider two p_{isol} values (0.5 and 0.9) as 'low' and 'high' isolation rates, noting the likely caveat of reporting biases. Staff reported large numbers of daily contacts (mean 15.0) at their place of work, which, tallying with the results of consultations, we interpreted as a result of repeated interaction within a work cohort (with only rare random interactions on top). Hence our assumed cohort size for drivers of ≈ 13.

B. Workplace Network Model

In this section we present an overview of the model details, with further details supplied in appendix B. The model we use is a stochastic agent-based network model of disease transmission. The parameters and symbols used in the following section are all described in table I.

TABLE I: Model parameters for workplace contacts and transmission. The values given are the values used unless otherwise stated for a given figure or section. The "perceived uncertainty" is simply to indicate the level of confidence we have in the parameter values – Low: based on primary data or peer-reviewed sources; Moderate: based on literature reviews, surveys, or specific consultation questions; High: assumed or extrapolated from consultation answers.

Parameter	Description	Value	Source	Perceived uncertainty
N_D, N_L, N_O	Total number of drivers, pickers, and office staff employed in the workplace respectively.	Parcel: $\{50, 25, 15\}$ Large-item: $\{20, 10, 5\}$	Company data and consultation	Low
T_D, T_L, T_O	Total number of driver, picker, and office staff cohorts/teams.	Parcel: $\{3, 2, 1\}$ Large-item: $\{2, 2, 1\}$	Consulations and survey	Moderate
$n_D(t)$, $n_L(t)$, $n_O(t)$	Number of drivers, pickers, and office staff working on day t respectively.	Variable	Company data and consultation	Low
$D_P(t)$	Total number of packages delivered on day t.	Variable	Company data	Low
p_c	Probability of two individuals at work having a random F2F contact in a given day.	$2/(N_D+N_O+N_L)$	Consultation and survey	High

ρ_D	For contacts including drivers, p_c is scaled by this factor.	0.05	Consultation	Moderate
f_c	Cohort flux rate. The probability each day of a worker switching to a different cohort.	0.01 per day	Consultation	High
β_{F2F}	Infection rate for F2F contact at 1m distance while speaking (with a person with unit infectiousness)	0.15 h^{-1}	A plausible range of 0.03–0.24 was inferred from [22–24]	Moderate
c_i	Modifier for exposure due to type of contact i	1 (inside, talking) ×0.2 (outside) ×0.2 (not talking)	[22]	Moderate
β_{SS}	Infection rate via room-sharing (with a person with unit infectiousness)	0.002 h^{-1}	See appendix D 1	High
x_{ss}	Effective distance for room-sharing interaction	4.3m (shared spaces), 3.6m (office)	see D 1	Moderate
β_{FOM}	Package-mediated fomite infection rate (from a person with unit infectiousness) if time between handling is 0.	0.001 per contact (UOS)	Assumed	Very high
λ	Half-life of virus deposited on packages.	3 h^{-1}	[25]	Low
τ_{office}	Time office staff spend in shared office each day.	6 h	Consultation	Low

τ_{break}	Time office and picker staff spend in shared break rooms	1 h	Consultation	Moderate
H	Average number of employees per employee household minus 1 ($H = 0$ means no employees live together, $H = 1$ means the average household has two employees)	0.05, 0.5	Assumed	High
C	Number of cars/shared commutes per households minus 1.	0.05, 0.5	Assumed	High
$J_k[V_k(t - t_k])$	Relative infectiousness of person k with viral load V_k infected at time t_k.	See appendix A 3	[26]	Moderate
$S_k(t - t_k)$	Relative susceptibility of person k infected at time t_k.	$S_k(t - t_k < 0) = 1$ $S_k(t - t_k \geq 0) = 0$	Basic SIR model assumption	Low
p_{symp}	Probability that an individual develops symptoms relevant for self-isolation guidance.	0.5	[3]	Moderate (is age, variant, and guidance dependent).
p_{isol}	Probability that an individual adheres to self-isolation guidance.	0.5, 0.9	[21] and Survey	Moderate.
p_{miss}	Probability that an 'adherent' person misses a test.	0.4	Data from other sectors	Moderate.

The model considers contacts between all employees working in a home delivery depot

(i.e. engaged in business-to-consumer delivery or B2C) that has a warehouse and onsite offices. The workplace is populated by 3 groups: drivers, who deliver packages from the warehouse to customers; pickers, who transport and load packages within the warehouse; and office/admin staff, who work in the same building but in shared offices. There exists a pool of N_D drivers , N_L pickers and N_O office staff available for work each day. Workforce turnover is ignored, as it is assumed negligible over the time scales considered, however it may play a role over long time periods.

1. Employee work schedules

The model network consists of all within-workplace contacts between employees, as well as contacts between employees due to house-sharing or carpooling, in order to simulate workplace outbreaks in detail. Thus we assume, unless they share a household, employees only make contact with other employees if they are both at work on that day. We use an idealised model for the work schedule, whereby the number of employees in work depends on the day of the week, this pattern was calculated from data from two UK logistics firms (see Appendix A for details). For all pickers and drivers, we randomly assign consignments (i.e. deliveries/packages) for loading and delivery (as detailed in Appendix A). We assume that each consignment is first handled by pickers, then subsequently by drivers, and finally by the customer. Drivers are the only group of employees that have direct contact with members of the public while on shift. For simulation efficiency, repeat interactions with customers are not considered (as contacts via this route have a very low probability of infection, so double counting of infections is very unlikely), but these contacts are simulated and infection ingress/egress through this route is included in the model.

We also consider the case where drivers and pickers work in pairs (i.e. large goods delivery), we round the number of staff required in these roles to the nearest even number, and then assign pairings randomly each day. One intervention simulated is fixed pairings; in this case, these are assigned a priori and we pick the pairs working on a given day at random from those available. A pair is unavailable if either worker in that pair is isolating, therefore this intervention is always used alongside "pair isolation", where one member of the fixed pair isolates for the same period as their partner (whether or not they develop symptoms).

2. Workplace contacts and infections

Infections are modelled to occur via four routes; face-to-face (F2F) contact with infectious individuals, indirect contact via sharing a space with infectious individuals, household sharing, and fomite transmission via goods handling.

The model generates direct F2F contacts between employees through three different mechanisms, summarised in table II. Table II also lists the parameters for the different contact routes simulated. Contacts made via these routes are assumed to be dominated by face-to-face transmission (see appendix A 4 for simulation details).

Indirect aerosol-mediated transmission is taken to occur on a one-to-all basis. Given the well-ventilated nature of warehouses, we assume that this kind of transmission only occurs in offices, or in lunch/break rooms. Finally, fomite transmission via package handling is simulated as a decaying random process, such that the probability of onward transmission depends on the time between package handling events by infectious and susceptible individuals. The details of how these routes are simulated is given in appendix A 4.

The transmission routes between different groups are illustrated in fig 1.

C. Individual characteristics: viral load, infectivity, and test positivity

Viral load trajectories are generated from the individual level data in [26]. The algorithm to generate individual viral load and infectiousness profiles is described in further detail in appendix B and in [27] is available at [28]. It is summarised in appendix A 3, with values given in table III.

D. Simulation algorithm

We simulate two types of scenario:

- **Point-source outbreak:** A single index case is chosen and we assume that there are no other introductions during the simulation. All other employees are susceptible at the simulation start (i.e. zero prevalence). The simulation terminates when there are no infectious cases remaining. This type of scenario is modelled in section III A and in appendix sections C 0 a–C 0 c.
- **Continuous-source outbreak:** No index cases are chosen initially and introductions occur randomly (Poisson process) based on the community incidence and prevalence

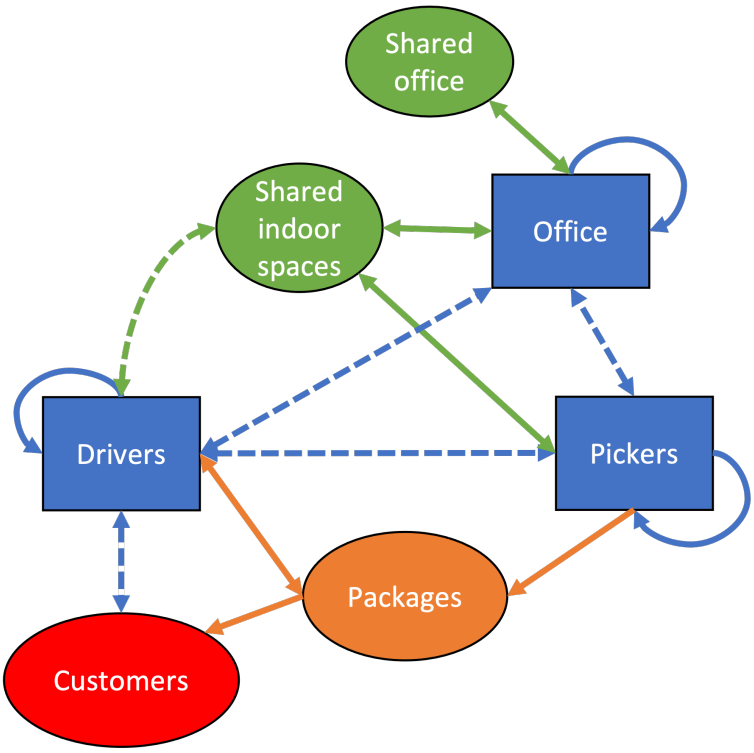

FIG. 1. Sketch of workplace staff groups and the potential transmission routes between them. Blue lines indicate face-to-face contacts, with dashed lines indicating transmission routes with either a lower contact rate or less contact time. Orange arrows are fomite transmission routes (via packages) and green indicates aerosol transmission in shared rooms. Arrows indicate direction of transmission.

in March-June 2020. The simulation runs for a fixed time window, and the number of customer contacts and packages delivered follow the pattern of demand experienced during that period of time (see appendix A). This scenario is modelled in section III A 1.

In the point-source outbreak scenarios, in order to define a 'successful' outbreak we arbitrarily set a threshold of a final attack rate of 5%. Note that we choose this as it is a low-threshold, like the epidemiological definition of an outbreak as a single linked secondary case. However, by defining it as a percentage of workplace size this makes the results from the two different settings more comparable. Therefore, if $R - 1 > 0.05(N_D + N_L + N_O)$, where R is the number of recovered individuals at the end of the simulation, then we record this simulation as a successful outbreak. The fraction of simulations where a successful outbreak occurs is then used as an estimate of the probability of an index case resulting in an

outbreak.

For continuous-source outbreaks, there is random ingress of new cases, so instead we compare the number of workplace infections (ignoring introductions) as well as the number of isolation days to measure impacts on productivity. Introductions can occur in these simulations through two routes:

- **Community ingress:** Each susceptible individual in the workplace has probability $I(t)$ of being infected outside of work, where $I(t)$ is the community incidence at time t.

- **Customer ingress:** For each delivery a driver makes, there is probability $P(t)$ that the customer is currently infectious, where $P(t)$ is the community prevalence at time t. When a susceptible driver interacts with an infectious customer, there is probability $p_{\text{cust}} = 1 - \exp(-c_i \beta_{F2F} \tau_{\text{doorstep}})$ of an infection.

This is a very simple model of case ingress and does not account for household structure, the geographical/individual variability in the wider population, or repeat deliveries to customers.

The testing strategy we model here is non-directed mass testing, i.e. all employees are tested regularly every τ_p days. A random day in the period $[1,\tau_p]$ is drawn as the first test day, and all subsequent test days follow sequentially τ_p days after the previous. Following a positive test, an individual cannot be tested again for τ_{pause} days after their positive test. Other testing strategies may be beneficial, particularly if looking to reduce the burden on employees or because of affordability, and we address some of these in the discussion.

The simulation follows an SIR-type structure, such that individuals who have previously been infected cannot be re-infected. This is a reasonable assumption over the timescales of up to 3 months that we consider here. An example visualisation of a single realisation of the simulation is shown in figure 2. The source code for the simulations can be found at [29].

III. RESULTS

Appendix C contains results pertaining to the baseline transmission dynamics in the two work settings that we focus on. This includes an investigation of changing parameters that affect the mixing rates in the settings, including changing work cohort size and close-contact work in pairs. This shows that, in the parcel workplace, we predict that office size and occupancy is a more important potential factor in workplace outbreaks than transmission between drivers at the workplace, even though office workers are in the minority (section

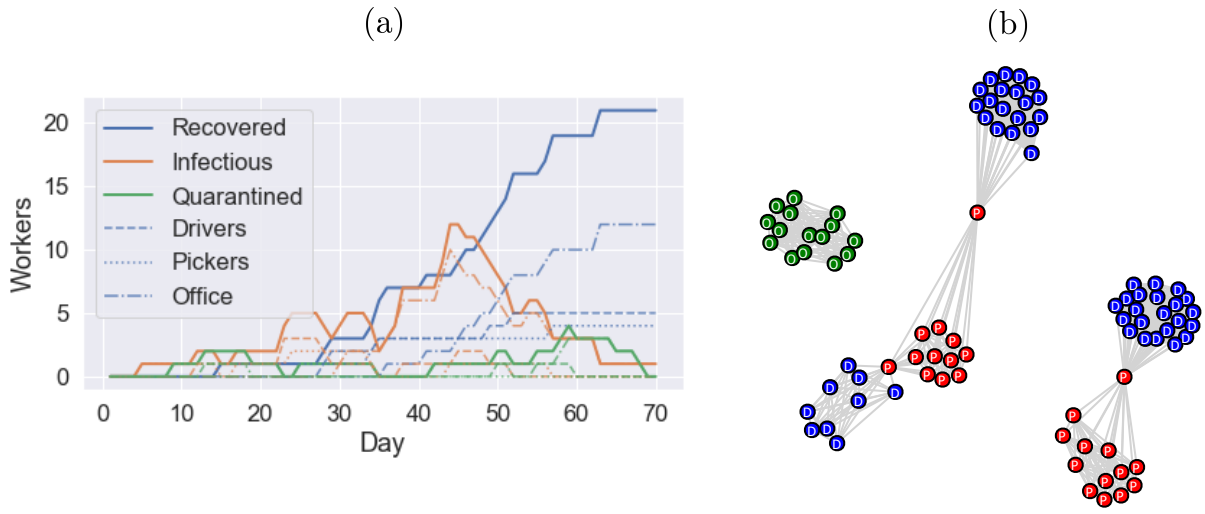

FIG. 2. Example outbreak in a parcel delivery workplace, where the simulation terminates when no infectious cases remain. (a) The evolution of the number of recovered, infectious and quarantined (isolated) people in the model on each day (dashed and dotted lines indicate the same quantities for each subgroup as labelled). (b) Example network of the "cohort" contacts, each cohort has edges between all member nodes, additionally each driver cohort (blue D nodes) is supervised by a member of staff from the warehouse (red P nodes). Office staff are disconnected (green O nodes), but make contact through random interactions, break rooms, and house/car sharing arrangements.

C 0 a). In the large-item delivery workplace, close-contact working pairs (primarily delivery pairs, who share a vehicle for much of the day) were predicted to be very important, and keeping these pairs fixed had a significant impact on reducing workplace spread (section C 0 b). Finally, we also present the effect of presenteeism, which in this model we define as workers with symptomatic COVID-19 attending work, which we find can have a notable effect on transmission, particularly when coupled with other measures to isolate close-contacts of symptomatic individuals (section C 0 c).

Furthermore, appendix D contains a sensitivity analysis of some of the pertinent baseline model parameters, to show how these affect predicted transmission rates.

In this following section, we focus on the impacts of testing and the combination of different workplace interventions to analyse their potential effectiveness.

A. Impact of mass testing on point-source outbreaks

Given the long incubation period of COVID-19 (compared to flu) and the significant proportion of asymptomatic cases, regular mass testing has been proposed and deployed in various settings to screen asymptomatic and pre-symptomatic cases. Figures 3 and 4 show the reduction in outbreak probability resulting from testing at different frequencies with different test types in the parcel and large-item delivery work settings respectively. Overall, the results show that even with a 2-day turnaround, PCR has a bigger effect on transmission that LFD tests, due to the increased sensitivity, however the effect of LFD tests is still significant considering their relative low cost. Note this estimate for the sensitivity of LFD tests is lower than some previous models [20, 30, 31] as it is based on data from self-swabs in a real-world setting rather than lab data.

In each figure, two cases, representing idealised behaviours, are shown. In the first case testing is voluntary meaning 90% of people do 60% of the required tests on average, while the other 10% do no tests (3(a) and 4(a)). This therefore reduces the potential benefits of testing. In the second case testing is enforced(3(b) and 4(b)) meaning that all workers test and report their results. This is the theoretical maximum effect that we could expect testing to have.

Comparing figures 3 and 4 shows that testing has a greater proportional impact in the large-item delivery delivery setting. Furthermore, in this case testing can still have a noticeable effect even when performed as infrequently as 14 days. With total compliance to testing, the probability of outbreaks in the large-item workplace model is reduced by approximately 50-60%, and around 40-50% in the parcel model by twice weekly LFD tests (which have been deployed in other sectors). The reason for this difference is the same as in the previous section on presenteeism, namely the combination with the fixed-pair isolation intervention in the large-item delivery setting.

To conclude, we have found that regular testing, particularly in combination with close-contact isolation, can have a very significant effect on workplace transmission. Any testing intervention needs to be weighed against potential costs, at low community prevalence the vast majority of tests are likely to be negative, and those that are positive are more likely to be false positives and so the intervention may not represent good value for money. Alternatively, at high community prevalence, testing and close-contact isolation could result in many isolations, some of which are only precautionary, which can have a huge impact on business. The latter case is not well described by the point-source outbreak considered in

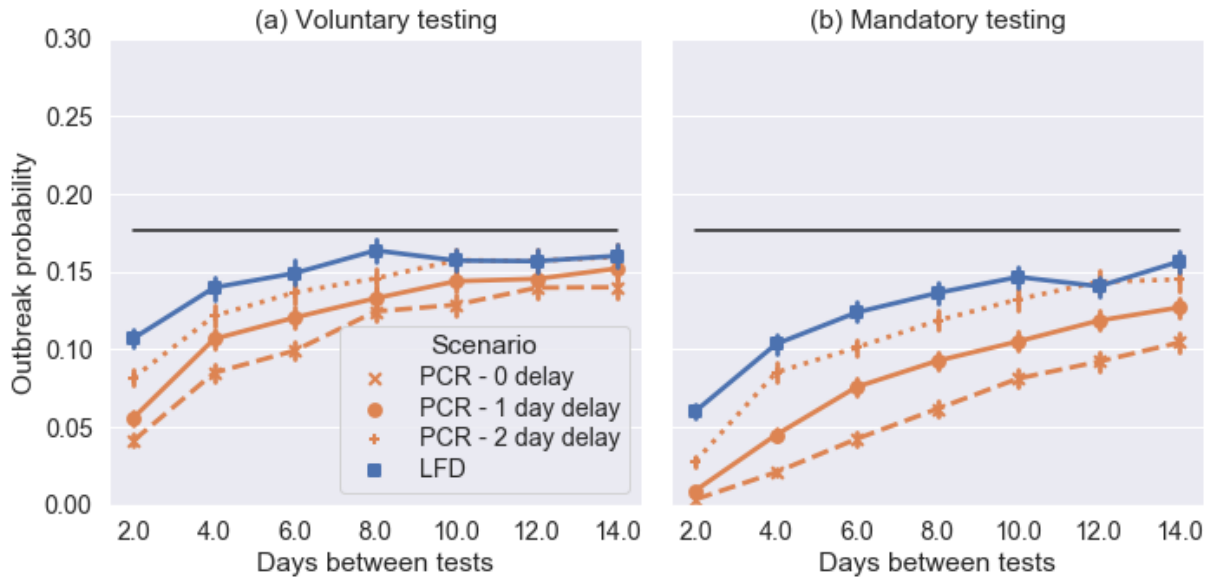

FIG. 3. Probability of an outbreak in the model parcel delivery workplace from a single introduction (selected at random), where the black line is the mean baseline case (no testing, estimated from 10,000 simulations). Each coloured marker shows the mean result of 10,000 simulations with the labelled testing intervention. In (a) testing is not enforced so $p_{\text{miss}} = 0.4$ and and in (b) it is so $p_{\text{miss}} = 0.0$ and all people isolate with a positive test. In both cases we use $p_{\text{isol}} = 0.9$ for symptomatic isolation.

this section, as introductions into the workplace are more likely to occur in quick succession. Therefore in the following section we look at the impacts of a range of interventions in the case of a continuous-source outbreak.

1. *Impact of interventions in a real-world context*

In this section we model each workplace in the context of realistic community SARS-CoV-2 incidence rates. We used incidence rates inferred from deaths and hospitalisations in the UK during the period 1st March 2020 until 31st May 2020 (see appendix A 2). We then applied ran simulations with different interventions in place, for each scenario we added an extra intervention to the ones applied before, the interventions are:

1. Symptom isolation only: People who develop symptoms self-isolate with probability $p_{\text{isol}} = 0.5$.

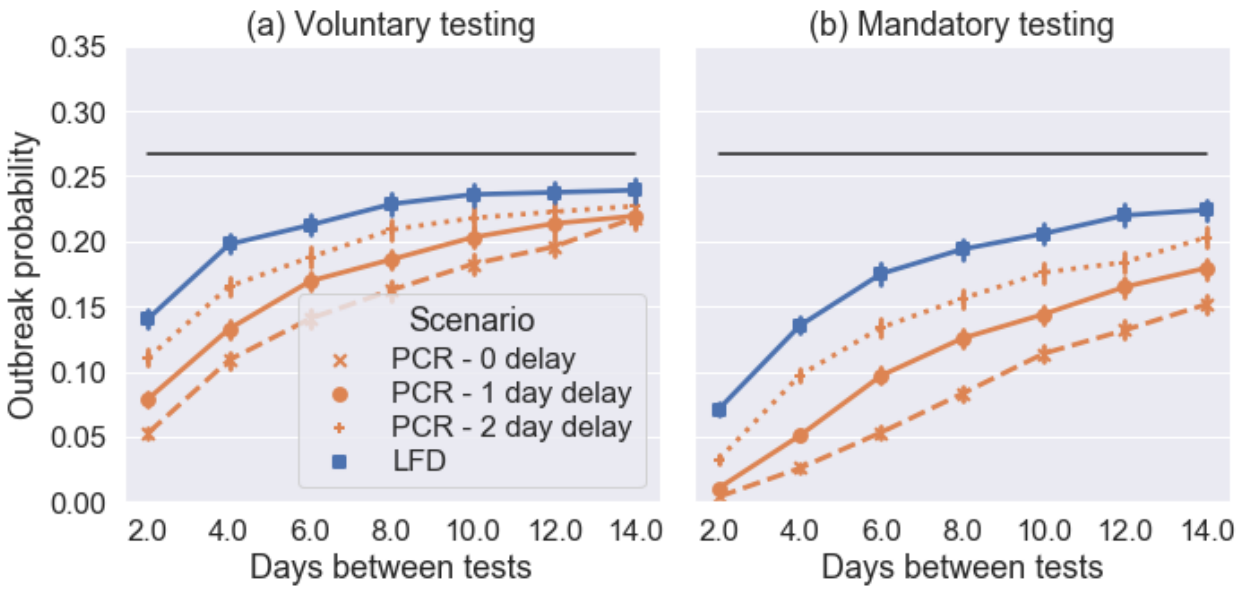

FIG. 4. The same as figure 3 but for the model large-item delivery workplace with fixed pairings and pair isolation in place.

2. Improved isolation: To mimic the impact of pandemic messaging, isolation probability is increased to $p_{\text{isol}} = 0.9$.

3. Distancing: All F2F interactions, except those involved in pair work, have interaction distance $x = 2$m.

4. Cohort Size Reduction: In the parcel delivery setting, the number of cohorts for all job types is doubled.

5. House share isolation: All employees who share a household isolate when one self-isolates.

6. Fixed-pairings: In the large-items delivery setting, driver and picker pairs are fixed and both self-isolate if one self-isolates.

7. Office WFH: Office staff do not enter work, they only make contact other employees if they share a household.

8. Testing: Twice weekly lateral flow testing is introduced for all employees.

9. Enforced testing: Testing becomes mandatory so no tests are missed.

10. Car share isolation: If a person travels to work with someone who self-isolates, they self-isolate.

11. Cohort isolation: If one member of the cohort isolates, all people in the cohort isolate.

In the model, introductions due to customer interactions only had a small but noticeable effect meaning that drivers were slightly more exposed than other employees (mean 0.11 introductions per driver for both work settings, averaged over all scenarios vs. 0.09 for other staff respectively). Nonetheless, over the period, around 10% of the workforce is infected purely due to the imposed prevalence and incidence.

Figure 5 shows the cumulative impact of interventions on secondary cases and isolations in the parcel delivery workplace. The interventions are applied in approximately the sequence that was reported by companies we consulted. The intervention "Distancing" increases all "cohort" and "random" contacts to 2m interactions and has a large effect. Reducing cohort size and office staff working from home ("Office WFH") have a big impact on reducing transmission since this model predicts that outbreaks are most likely to start in this group. Interventions beyond "enforced testing" are predicted to increase isolation levels without much greater impact on transmission, particularly "cohort isolation" which likely causes a great deal of disruption despite these groups being unlikely to be infected. Note this becomes a much more viable option though if cohorts are much smaller, which is one major benefit of reducing cohort size if possible. Comparing the two graphs in 5 we see that is a slightly more efficient to have contact reduction measures in place before adding isolation-based measures, as these reduce the number of workers who will need to isolate. When isolation measures are implemented alone, we see an increase in the predicted number of isolations even though the relative reduction in transmission is similar.

The impact of interventions for the large-item delivery workplace is very similar (see figure 6). We see that the "fixed pairings" intervention (which includes pair isolation) has a marked effect on transmission. The extra benefit gained from testing is clearly visible too, but again isolation measures beyond this appear have little further effect.

To conclude, figures 5 and 6 demonstrate some of the trade-offs for different intervention measures in terms of their impact on transmission and their impact on the number of isolating employees. Certain interventions act to reduce both (social distancing, Office staff WFH) but potentially have other costs for business/feasibility issues that need to be considered. When there are employees that still need to be in close-contact (e.g. driver and picker pairs in this model) the combination of fixed pairings, pair isolation, and regular testing is highly effective

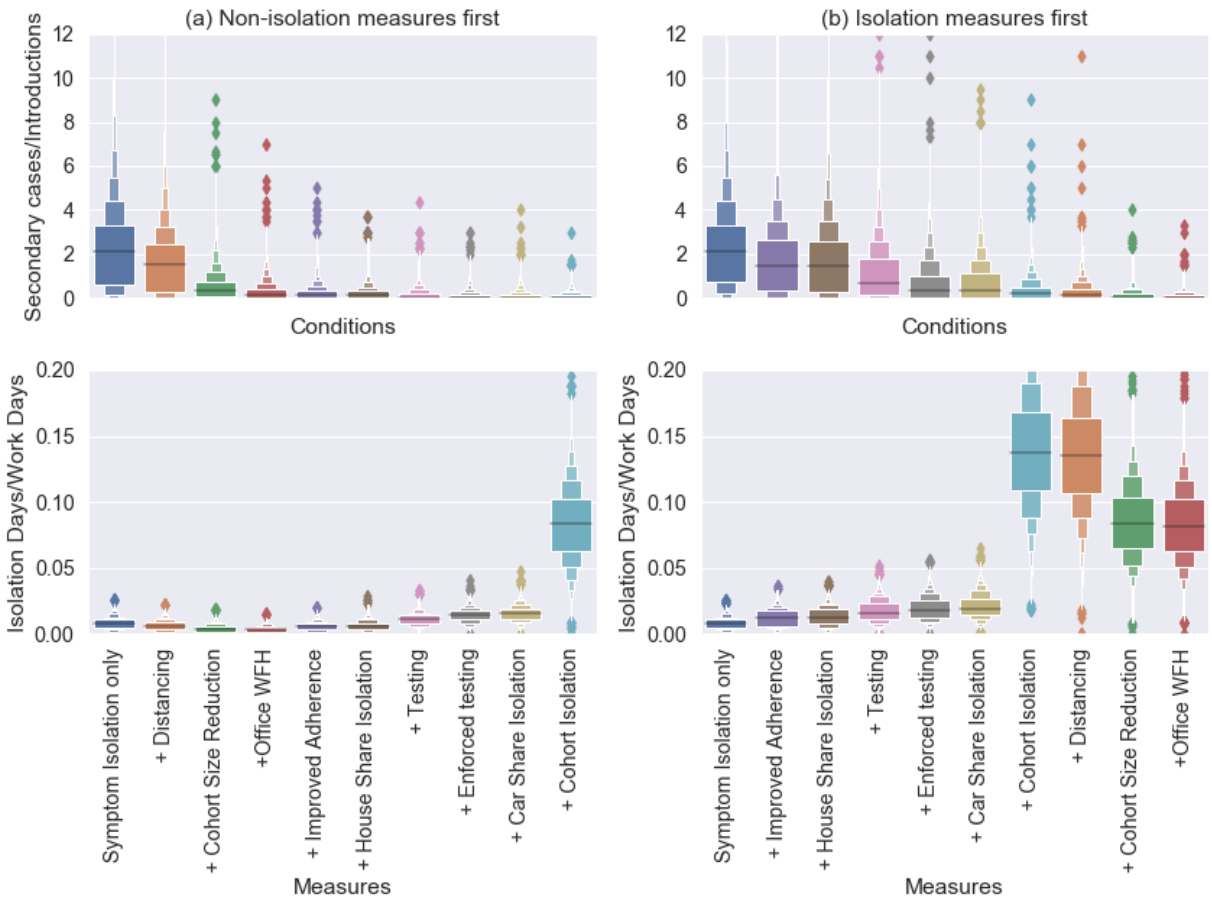

FIG. 5. Boxen plots of the number of secondary cases divided by the number of introductions in a parcel delivery workplace over a 3 month period. Each distribution shows all the simulations (from 10000) with more than one introduction. The labels on the x-axis indicate the addition of an intervention (in-tandem with all the interventions to the left). In (a) the measures restricting contacts are introduced first and in (b) the isolation-based measure.

for reducing transmission. However, in cases where there is high rates of household-sharing (or, more generally, any contacts between employees outside of work during isolation) then this can continue to drive transmission between employees and is difficult to distinguish from workplace transmission.

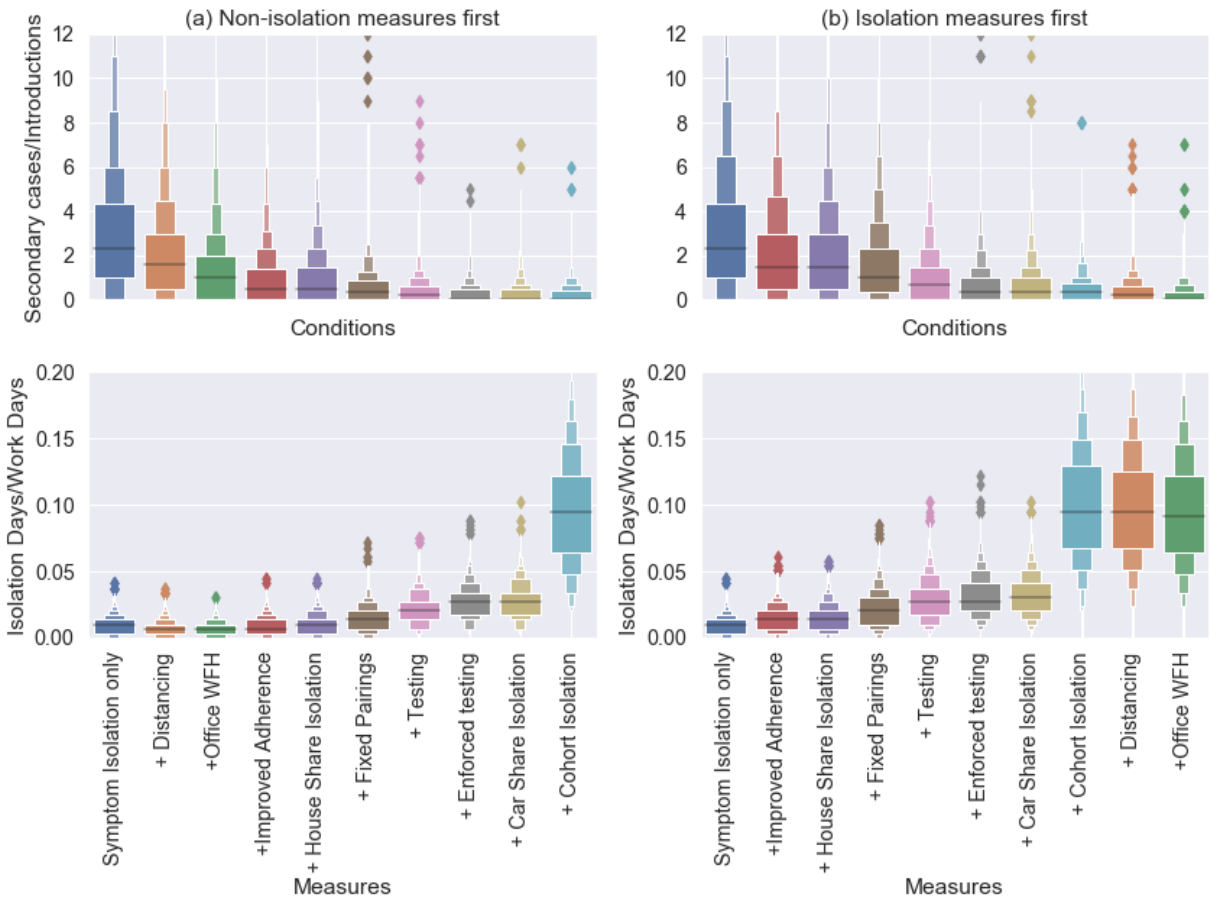

FIG. 6. The same as figure 5 but for the large-item delivery workplace.

IV. DISCUSSION

In this paper we have developed a stochastic model of SARS-CoV-2 spread in small/medium size workplaces. The contact patterns simulated were designed to represent warehouses/depots in the home-delivery sector, particularly those focusing on B2C delivery. To our knowledge this is the first model to consider SARS-CoV-2 transmission in this sector specifically. While the parameterisation of these models has significant uncertainty, we have been able to test the relative impact of various interventions that companies in this sector deployed to reduce SARS-CoV-2 transmission over a range of scenarios and parameter regimes.

The results predict that workplace transmission in this sector is modest, due to drivers working alone most of the day, and warehouse staff working in large open environments. Without any interventions there is predicted to be a small risk to customers for an indi-

vidual delivery, but in workplaces undergoing an outbreak, home-installation of items can pose a significant risk to customers without interventions. The companies we consulted discontinued home-installation during in the spring of 2020, but later re-introduced it with social distancing measures. Parcel delivery companies have switched to "contactless" delivery, meaning that signatures are no longer required, essentially eliminating the only route of transmission to customers. Overall, this suggests that this sector played a key role in reducing community transmission of SARS-CoV-2, as it allowed people to stay at home during periods of high-prevalence. Quantifying this impact is more difficult though as the counterfactual situation (i.e. how people would have behaved if this sector failed to keep up with increased demand) is unknown.

Safeguarding the key workers in this sector was a broader challenge and companies reported implementing multiple measures based on government guidelines and their own judgement. A key result of this paper is the finding that the potential impact of self-isolation and testing policies is dependent on how much transmission between employees occurs in work vs. at home. Thus, identifying high-risk contacts (due to e.g. shared accommodation or work tasks requiring prolonged close-contact) is very important and forms the basis of contact-tracing interventions. Workplaces have an extra advantage over contact-tracers in that they have control and knowledge over some of the contacts that employees are required to make in their line of work. Therefore, high-risk contacts can be limited by using fixed pairs for large-item delivery, reducing then number of people sharing an office, and reducing the occupancy in shared spaces. This then allows efficient isolation policies to be implemented based on knowledge of the limited number of high-risk contacts people have made (e.g. workers are given paid isolation leave if they share accommodation or work in a delivery pair with an employee who has tested positive or reported COVID-like symptoms). Figures 12 and 4 show that this combination can be extremely effective in small workplaces.

Rates of presenteeism, which in this case we define as those who do not self-isolate when they develop symptoms, has been shown to be much less likely if fully-paid sick leave is offered [32, 33]. Therefore, in order to be effective, such isolation policies could incur considerable costs to a business as well as reducing productivity. Similarly, company-backed testing and isolation interventions will incur further costs and mean that asymptomatic cases are detected, potentially resulting in even more isolations. Therefore, companies may be apprehensive about deploying such strategies. Here, we showed that these strategies are much more efficient when close-contacts of index cases can be identified and isolated too, particularly when such contacts are necessary for the job. This can mean that chains of transmission

are quickly shut down, and outbreaks are much less likely to occur. Furthermore, combining these measures with social distancing, WFH, and similar interventions that reduce transmission (e.g. masking) can reduce the number of isolations since workplace outbreaks become less likely.

The model developed has several limitations which are important for the interpretation of the results presented. First, the contact model has been developed based on a mix of quantitative (survey data, staff numbers and demand levels) and qualitative data (consultations). Novel insight was gained by speaking directly to representatives from the sector, but their position was not objective and so there may have been implicit biases in the descriptions of the nature of workplace contacts and some potential routes of infection contacts could have been missed. Furthermore, simplifying assumptions, such as all contact durations being identical for the same mode of contact, mean that this model is idealised compared to reality. Third, the transmission rate and the modifiers used for different types of contact are uncertain, and is based on a combination of peer-reviewed [23, 24, 34] and non-peer-reviewed literature [22]. Improvements to this transmission model from the adaption of more mechanistic modelling approaches that predict explicitly the infectious dose associated with different modes of contact [24, 34–41], as well as updating with data on new variants and vaccines, will mean that this model could be applied to numerous future workplace scenarios to test the impact of different non-pharmaceutical interventions.

There are also some complicating factors we choose to ignore in this model, that may be important to consider when interpreting these results. First, we do not model severe illness, which can impact results by increasing the time away from work of individuals with COVID-19. Second, we do not model the complex relationship between interventions and behaviour. It is possible that as more interventions are introduced, adherence with other interventions wanes so the expected impact of combined interventions may not be as high as predicted. This behavioural change is difficult to predict, and so would need to be monitored by companies to gauge whether interventions are working as expected.

One major benefit of the model presented here is that it incorporates the dynamics and variability in individual viral load, and simulates its impact on test sensitivity and infectivity. This, means that the correlation between test-positivity and infectivity is incorporated, meaning that impacts of these interventions can be more accurately estimated. Thus we were able to estimate not only the effect on average transmission rates, but also the frequency of rare superspreading events. This has highlighted the importance of stacking interventions that reduce transmission through different mechanisms. The source code is open access [29]

and the underlying network transmission model is malleable enough to be applied to any small closed populations.

In conclusion, this paper has shown that the multiple interventions put in place by the logistics and home delivery sector during the early stages of the pandemic are likely to have reduced the risk of community and workplace transmission by safeguarding customers and staff. The availability of lateral flow tests is another valuable layer of protection that could be added, and that this would most effective when combined with isolation measures that target the most high-risk contacts.

Appendix A: Sector-specific data collected and derivation of parameters

1. Staff and delivery numbers

To obtain realistic figures for the workplace size and number of consignments, we received data from a parcel delivery company and a logistics company that deliver large items, both in the UK.

From the parcel company, we received company-wide figures for number of consignments (i.e. delivery drops) and number of drivers on-shift from 01/01/2020 to 01/09/2020. First, we fitted a linear generalised additive model (GAM) to the number of consignments, in order to extract a smoothed curve $P^{(p)}(t)$ representing the demand over this period (see figure 7(a)). Next, we used negative binomial regression to extract the weekday dependence for both the number of drivers and the number of parcels. The model means (μ for drivers and λ for deliveries) were parameterised as

$$\mu^{(p)}(t) = \exp\left(\alpha_c^{(p)} + \alpha_p^{(p)} P^{(p)}(t) + \sum_{d=0}^{6} \alpha_d^{(p)} \delta_{d,w(t)}\right) \tag{A1}$$

$$\lambda^{(p)}(t) = \exp\left(\beta_c^{(p)} + \beta_p^{(p)} P^{(p)}(t) + \sum_{d=0}^{6} \beta_d^{(p)} \delta_{d,w(t)}\right) \tag{A2}$$

$$\text{where } w(t) = (t \mod 7), \tag{A3}$$

such that $w(t)$ returns the day of the week (Monday = 0, Tuesday = 1, etc.) and $t = 0$ is a Monday. The weekday dependence for each quantity is shown in 7(b). Finally, we were also provided with weekly data for each site (again for number of consignments and number of drivers). We again fitted a negative binomial regression to this data over the same period, with categorical parameters for each site to account for the differences in demand. The mean

of this model was parameterised as

$$\bar{\mu}^{(p)}(u,s) = \exp\left(\bar{\alpha}_c^{(p)} + \bar{\alpha}_p^{(p)} W^{(p)}(u) + \sum_{s'=0}^{N_s-1} \bar{\alpha}_{s'}^{(p)} \delta_{s,s'}\right), \tag{A4}$$

$$\bar{\lambda}^{(p)}(u,s) = \exp\left(\bar{\beta}_c^{(p)} + \bar{\beta}_p^{(p)} W^{(p)}(u) + \sum_{s'=0}^{N_s-1} \bar{\beta}_{s'}^{(p)} \delta_{s,s'}\right), \tag{A5}$$

$$\tag{A6}$$

where u is the time in weeks (e.g w/c 01/01/2020 is $u = 0$), $W^{(p)}(u)$ is the weekly demand (i.e. the total demand $P^{(p)}(t)$ summed over the days in week u) and s is the site number (indexed from 0 for all N_s sites).

Similar data was provided by a large-items logistics company. In this case, we were provided with daily data for the number of consignments and number of vans for each site in the company from 01/04/19 to 01/09/20. First, we fitted a linear GAM to the total number of consignments over all sites to extract a smoothed demand curve $P^{(l)}(t)$ (shown in 7(a)). Next, we fitted a negative binomial model to both account for weekday effect and site, with mean

$$\mu^{(l)}(t,s) = \exp\left(\alpha_c^{(l)} + \alpha_p^{(l)} P^{(l)}(t) + \sum_{d=0}^{6} \alpha_d^{(l)} \delta_{d,w(t)} + \sum_{s'=0}^{N_s-1} \alpha_{7+s'}^{(l)} \delta_{s,s'}\right). \tag{A7}$$

$$\lambda^{(l)}(t,s) = \exp\left(\beta_c^{(l)} + \beta_p^{(l)} P^{(l)}(t) + \sum_{d=0}^{6} \beta_d^{(l)} \delta_{d,w(t)} + \sum_{s'=0}^{N_s-1} \beta_{7+s'}^{(l)} \delta_{s,s'}\right). \tag{A8}$$

We assume that, in the absence of COVID isolations, staff numbers on average follow the same daily pattern as driver numbers shown in figure 7(b). The selection of employees in work for a given job j on a given day is a three-step process:

1. All workers in COVID-related isolation are removed.

2. Of those available, each is assigned a random absence with probability p_{abs} and removed from the availability pool.

3. Of those still available, each has probability $\exp\left(\alpha_{w(t)}^{(i)} - \alpha_{\max}^{(i)}\right)$ of being in work on day t, where $\alpha_{\max}^{(i)}$ is the negative binomial parameter corresponding to the day with highest occupancy. In this notation $i = l$ if in a large-item delivery workplace and $i = p$ is the parcel delivery workplace.

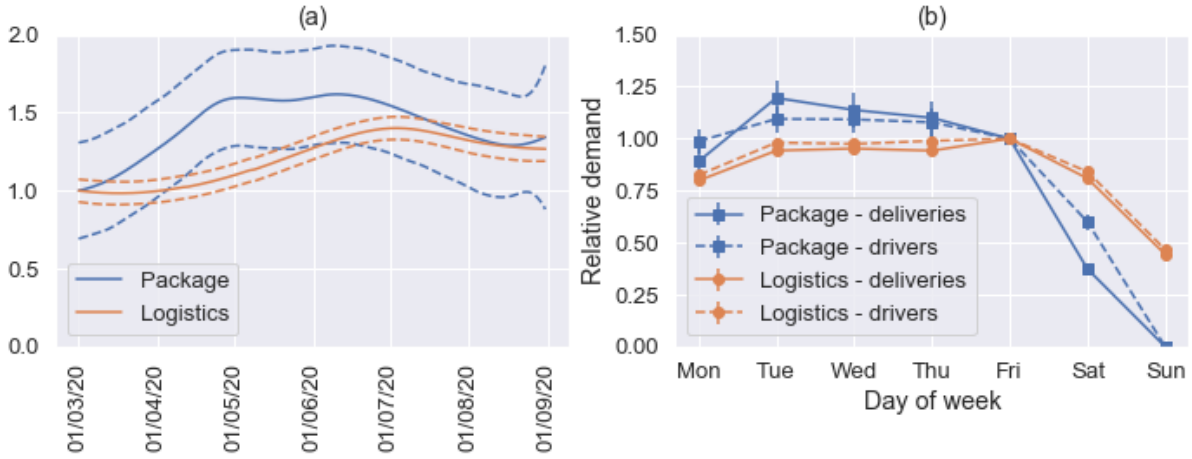

FIG. 7. (a) Smoothed demand curves, fitted using a linear GAM to company-wide figures for number of consignments, for the parcel and logistics companies. The figures are given relative to their value at 01/03/20. (b) Weekday dependence for number of drivers and deliveries fitted using negative binomial regression. Each point shows the number of deliveries or drivers relative to the number on a Friday.

The fitted weekday coefficients are used to model the day-to-day variation in the number of deliveries, so that for $i \in \{l, d\}$

$$D_i(t) = D_i^{(0)}(t) \exp\left[\beta_{w(t)}^{(i)}\right]. \tag{A9}$$

We use different values for the background demand $D_i^{(0)}(t)$ based on the type of simulation.

- Scenario simulation: For the parcel delivery workplace, the weekly negative binomial model can be used to approximate the number of deliveries over this period such that

$$D_p^{(0)}(t) = \bar{\lambda}^{(p)}(t, s_{\text{med}}^{(p)}) / \left\{ \sum_{d=0}^{6} \exp\left[\beta_d^{(p)}\right] \right\}, \tag{A10}$$

  where $s_{\text{med}}^{(p)}$ is the index of the median site in the parcel delivery dataset. In the large-item delivery workplace then $D_l^{(0)}(t) = \lambda^{(l)}(t, s_{\text{med}}^{(l)})$ where $s_{\text{med}}^{(l)}$ is the index of the median site in the large-item delivery dataset.

- Outbreak simulation: We assume fixed pre-pandemic levels of demand (approximately equal to the scenario simulation case at March 1st 2020). In this case we use $D_p^{(0)}(t) = 3000$ and $D_l^{(0)}(t) = 210$.

in the parcel and large-item workplaces respectively. In this way, $W_{\mathrm{p}}^{(0)}(t)$ represents the number of deliveries that the parcel workplace completes in a week. For outbreak simulations we fix this at

In the case of outbreak simulations, we fix $D_{\mathrm{i}}^{(0)}(t) = N_P$ where $N_P = 3000$ deliveries per week for the parcel company and $N_P = 210$ deliveries per week for the logistics company.

To make the number of staff in work each day consistent with the data for a median workplace, we defined the total number of drivers as

$$N_D = \left\lceil \frac{1}{7} \sum_{w=1}^{7} \frac{N_P}{p_{PD}(1 - p_{\mathrm{abs}})} \exp\left(\beta_{\mathrm{P-DOW}}^{(w(t))} - \beta_{\mathrm{S-DOW}}^{(w(t))} + \beta_{\mathrm{S-DOW}}^{(\max)}\right) \right\rceil, \tag{A11}$$

where p_{PD} is the average number of parcels delivered per driver per day under normal conditions (85 for parcel delivery and 15 for large-item). The number of warehouse and office staff were then defined relative to this.

In the in situ scenarios, we use the negative binomial fitted demand such that

$$D_{\mathrm{av}}(t) = \exp\left(\beta_c + \beta_p P^{(i)}(t) + \beta_{\mathrm{site}}^{(s_{\mathrm{med}})}\right) \tag{A12}$$

where $\beta_{\mathrm{site}}^{(s_{\mathrm{med}})}$ is the demand coefficient for the median site and $i \in p, l$ indicates whether it is the parcel or logistics company.

2. Community incidence and prevalence

The estimates community incidence data used for the continuous-source outbreak simulations are shown in figure 8. They are based on data on hospitalisations and deaths from 01/03/2020 – 31/05/2020 inclusive. Community prevalence was simply estimated as the cumulative sum of the incidence from the previous 10 days inclusive.

3. Viral load, infectivity, and test-positive probability

The viral load and infectivity trajectories are generated at random based on the mechanistic model fits in [26]. In order to use this data, we fitted the viral load trajectories with a piecewise exponential model

$$V_k(\tau) = \begin{cases} V_p \exp[r(\tau_p - \tau)] & \text{if } \tau \leq \tau_p \\ V_p \exp[-d(\tau - \tau_p)] & \text{if } \tau > \tau_p \end{cases} \tag{A13}$$

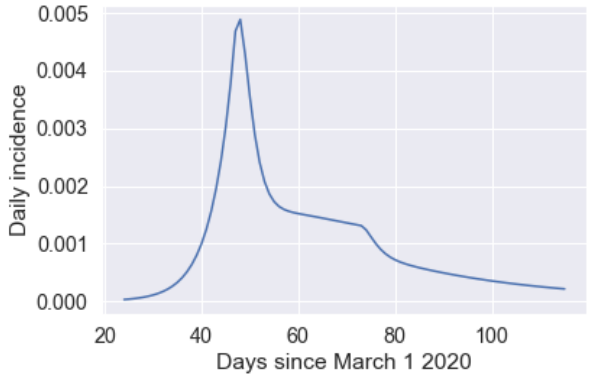

FIG. 8. Community incidence rates assumed for the continuous-source outbreak scenario.

where V_p is the peak viral load (in copies/ml), r is the exponential growth rate, d is the exponential decay rate, and τ_p is the time since infection to the peak viral load. These parameters are drawn from a multivariate distribution that is inferred from the data in [26]. The parameters of this distribution are given in table III.

There is probability p_{symp} of each individual developing symptoms that would be identified as symptomatic COVID-19. For those that do, symptom onset time is drawn from a gamma distribution (see table III for parameter values), which is truncated so that symptom onset occurs within ± 2 days of peak viral load [42, 43].

In order to model infectivity, we use "infectious virus shed" as fitted in [26] as a proxy. The infectious virus shed is a Hill function of viral load

$$J_k(V_k) = \frac{J_p V_k}{V_k^h + K_m^h}. \tag{A14}$$

We fitted a bivariate lognormal distribution to the random parameters of this model (J_p, h), given in table III. Note that, in [26], the magnitude of J_p is given in arbitrary units. In order to make this consistent with the transmission rate used here, we scale the distribution of J_p such that the population mean infectivity over the average duration of infection is 1.

The probability of testing positive is also assumed to be deterministically linked to viral load. To model PCR testing, we use a logistic function with a hard-cutoff to account for the cycle-threshold (Ct) cutoff

$$P_{\text{PCR}}(V_k) = \begin{cases} 0 & \text{if } V_k < V_{\text{cut}} \\ P_{\max}\left[1 + e^{-s_t(\log_{10} V_k - \log_{10} V_0)}\right]^{-1} & \text{if } V_k \geq V_{\text{cut}} \end{cases}. \tag{A15}$$

To model LFD testing, we use data from regular LFD and PCR testing in the social care sector in the UK. Since this data is based on positive PCR results, we assume $P_{\text{LFD}}(V_k) = theta(V_k)P_{\text{PCR}}(V_k)$. The parameters of these testing models are given in III.

Finally, individuals then have probability p_{isol} of being an "isolator", meaning that if they develop symptoms or test positive they will isolate. For "non-isolators", we assume these individuals do not participate in voluntary testing, but do participate in mandatory testing. In voluntary testing, those that do participate have probability p_{miss} of missing a test.

4. Transmission rates

A contact of type i between an infectious individual k and a susceptible person k' is assumed to have transmission rate

$$\gamma_{k,k'}^{(i)} = \beta_{F2F} c_i S_{k'}(t) J_k(t) \tau_i / 2^{x_i - 1} \tag{A16}$$

where β_{F2F} is the average transmission rate for face-to-face contact while talking at 1m separation, c_i is the transmission modifier for the type of contact, taken from [22], τ_i is the contact duration, and x_i is the contact distance in metres. $S_{k'}$ and J_k are the susceptibility and infectivity of individuals k' and k respectively on day t.

The baseline transmission rate β_{F2F} is estimated using multiple sources. First, in the [22], the probability of transmission while talking at 1m separation for one hour is given as 0.06 for the original SARS-CoV-2 virus and 0.15 for the delta variant. This suggests a β_{F2F} of 0.07^{-1} or 0.15^{-1} respectively. Test and trace data [23] suggests a workplace/school secondary attack rate of $\sim 3\%$ between close contacts, defined as either $<$ 1m for more than a minute, 1-2m for $>$ 15minutes or sharing a vehicle/skin-to-skin contact. If we take the average contact to be between 1-2m for 15-60min this gives a plausible range of β_{F2F} =0.03–0.24h^{-1}. Finally, in [24] the probability of infection while talking at 1m separation for 15 mins is ~ 0.03, suggesting a β_{F2F} of 0.13h^{-1}. Therefore, we take $\beta_{F2F} = 0.15\text{h}^{-1}$ in this model as a "best guess" from this range of estimates.

For household contacts, we use the transmission rate (per day) of

$$\gamma_{k,k'}^{(HH)} = \beta_{HH} S_{k'}(t) J_k(t) \tag{A17}$$

where $\beta_{HH} = 0.07$. This was set empirically using 10^6 realisations of infectivity trajectories so that the mean probability of household infections was 40% (approximately twice the observed household attack rate from the original SARS-CoV-2 strain [4, 22, 48, 49]). Comparing to

(A16), we see that this means the household transmission rate is approximately equivalent to 30 mins of F2F conversation indoors at a distance of 1m per day.

For package mediated fomites, we use a two-step process such that a fomite infection between workers occurs with probability

$$p_{kk'} = \exp\left[-(t_2 - t_1)\ln 2/\lambda\right]\left[1 - \exp(-\beta_{FOM} J_k(t_1) S_{k'} t_2\right] \tag{A18}$$

where $t_1 < t_2$ is the time the package is handled by an infectious individual k and t_2 is the time the package is handled by susceptible individual k'. The parameter λ is the half-life of the viable virus on the packaging, so the first exponential term represents this decay process. The second term is the same as used for all other contacts except that β_{FOM} is effectively the probability of transmission if an infected person handles a package that is then immediately handled by another employee.

Package handling is assumed to occur as follows

1. A picker (or picker-pair) k handles all of their l_k packages at times uniformly distributed in a time window of τ_L hours.

2. Each infectious packages n is then assigned a random integer r_n between 1 and P, which then determines which driver (or driver-pair) they get assigned to, such that $1 + \sum_{k'=1}^{k-1} d_k \leq r_n \leq \sum_{k'=1}^{k} d_k$ is assigned to driver k.

3. Drivers are assumed to handle all of their d_k packages twice. First they handle all at time τ_L, and second at times distributed between τ_L and $\tau_L + \tau_D$ (where τ_D the time is takes to complete all of the deliveries).

Finally, for shared-spaces (not including F2F contact), we use the dose-response relationship originally derived for SARS-CoV [50] and applied to SARS-CoV-2 [51]. Assuming that the number of aerosolised infectious plaque-forming units (PFUs) exhaled per hour is n_0, the concentration in the surrounding air (assuming fast mixing) will be

$$c(t) = \frac{n_0}{(\dot{f} + \lambda)V}\left[1 - e^{-(\dot{f}+\lambda)t}\right] \tag{A19}$$

where V is the volume of the room and $\dot{f}$ is the air exchange rate (air changes per hour, ACH), and $\lambda = \ln(2)/t_{1/2}$ is the decay rate of the aerosolised virions (such that $t_{1/2}$ is their half-life).

Therefore, the average concentration of infectious PFUs in the room while occupied by a single infectious person for duration τ is

$$\bar{c}(\tau) = \frac{n_0}{(\dot{f}+\lambda)V}\left[1 - \frac{1}{(\dot{f}+\lambda)\tau}\left(1 - e^{-(\dot{f}+\lambda)\tau}\right)\right] \tag{A20}$$

To convert this to a transmission rate, we assume that an average individual has an inhalation rate $\dot{V}_T$ (volume of air inhaled per hour). Their average dose, if sharing the space for the full period τ, is then $\dot{V}_T\bar{c}(\tau)\tau$.

The exponential dose-response model used in [50] has the same form as our infection model, so the transmission rate between individuals sharing the same space for period τ is given as

$$\beta_{ss} = \frac{\dot{V}_T\bar{c}(\tau)}{ID_e} \tag{A21}$$

such that the probability of infection via this route is $p_{ss} = 1 - \exp(-\beta_{ss}\tau)$. The infectious dose ID_e is highly uncertain, as is the dose exhaled n_0. However, the ratio n_0/ID_e is approximated in [34] as ∼16–18 per hour at peak infectivity. Given that, in our model, peak infectivity is ∼4 times mean infectivity, we use $n_0/ID_e = 4.0$ here.

In order to more directly compare this to the F2F interactions, we derive an "effective interaction distance" that is implied by this transmission rate. I.e. how far away would the two contacts have to be in a (no-talking) F2F interaction to experience an equivalent transmission rate in our model. This is given by $x_{\text{eff}} = 1 + \log(\beta_{F2F}/5\beta_{ss})$, since $\beta_{F2F}/5$ is the F2F transmission rate at 1m distance with the "no-talking" modifier. The parameters used to estimate x_{ss} are given in table IV.

a. Modes of face-to-face contact

We include several routes through which face-to-face contacts occur in the workplace, which are summarised in table II. Below we give some further details about how these are simulated:

- **Cohort contacts:** Daily F2F interactions between employees working the on the same shift and in the same area. For details of the rationale between how these cohorts are assigned, see Appendix A. It is assumed that, each employee contacts all others within their cohort for the same duration, such that the total face-to-face contact time for any given individual in a cohort is fixed. I.e. if a cohort consists of M people, each has a F2F contact with the other $M-1$ people in their cohort for $\tau_{\text{coh}}/(M-1)$.

- **Random interactions:** On a given day, each person with job j at work will randomly contact another employee with job j' with probability

$$p_{jj'} = \begin{cases} \rho_D p_c & \text{if } j = D \text{ or } j' = D \\ p_c & \text{otherwise} \end{cases} \tag{A22}$$

  The factor ρ_D is to account for the reducing mixing in drivers due to the time they spent not at the workplace during a shift. Note, $p_{DD} = \rho_D$ and not ρ_D^2 because we are assuming that drivers are on site at approximately the same time as each other.

- Explicit workplace pairings (includes **large-item handling**, **pair delivery**, and **pair delivery** routes): These are necessary for execution of picking and delivery of large items. When these pairings exist, all drivers and pickers are paired at the start of each shift, and this contact is guaranteed to occur during the shift. If the "fixed pairings" intervention is applied, then staff in pairs always have the same partners, otherwise the pairs are assigned randomly at the start of each day.

Appendix B: Simulation algorithm

At initialisation, the following model features are generated

1. Agents are assigned job roles and susceptible status.
2. The cohort contact network is generated as follows:
   (a) Within each job role, each agent is assigned a cohort at random.
   (b) For each driver cohort, one member of warehouse staff (a 'picker') is assigned to that cohort (representing a supervisory role).
   (c) Within each cohort, all agents are connected by edges with identical weight, which are active only when both agents are in work.
3. The house-share network is generated as follows:
   (a) $NH = \lfloor (N_D + N_L + N_O)/(1 + H) \rceil$ households are generated.
   (b) Each agent is assigned randomly to a household.
   (c) Within each household, all agents are connected by edges with identical weight that are active every day.

4. The car-share network is generated as follows:
   (a) $NC = \lfloor NH/(1+C) \rceil$ car-shares are generated.
   (b) Each household is assigned to a car-share, with all agents in that household assigned to the same car-share.
   (c) Within each car-share, all agents are connected by edges with identical weight that are active only when both agents are in work.

If simulating an outbreak scenario, an index case is infected on a random start day from Monday to Sunday. Upon infection, an agent is assigned the following:

- Viral load and infectivity trajectories.
- Symptom onset time.
- Adherence to self-isolation (true with probability p_{isol}).
- If testing: a test positive probability trajectory (section A 3).

The main simulation loop is executed for each day of the simulation, and proceeds as follows:

1. Update infectious state of all individuals moving any to 'Recovered' status who have reached the end of their infectious period.
2. Perform testing (if a testing day). For all positive tests generate an isolation time from the current day as $\lfloor \tau_d + u_{01} \rceil$ where $u_{01} \sim U(0,1)$ is a number uniformly distributed beteween 0 and 1, and $\lfloor . \rceil$ indicates rounding to the nearest integer.
3. Update isolation status for any who are due to isolate on this day.
4. Randomly generate any new introductions due to community incidence.
5. Select employees in work, all others are excluded from any workplace contacts for the rest of the day.
6. Generate all successful workplace infection events.
7. Generate customer infections and introductions.
8. Remove any infections where the infection target is not in the 'susceptible' state. For any viable targets that are subject to more than one successful infection event, select the recorded infection event at random.

9. Record all infection events, and for every individual infected change their status to 'infected' and their infection time to the current day.

10. Increment the day and return to step 1 unless the maximum number of days has been simulated. If an outbreak simulation and all individuals are in the 'recovered' state, terminate the simulation.

Appendix C: Baseline modelling results

At baseline (assuming all default parameters in table I, but high symptomatic isolation rate of $p_{\text{isol}} = 0.9$), our model predicts that the average number of cases the index case will infect is 0.181 ± 0.005, 0.934 ± 0.016, and 2.58 ± 0.03 when the index-case is a driver, picker, or office worker respectively. In the large-items delivery work setting, it is predicted to be 0.833 ± 0.012, 0.935 ± 0.015, and 1.608 ± 0.019 when the index-case is a driver, picker, or office worker respectively. Note that the error bounds here are 1.96 standard errors of the mean, and do not account for parameter uncertainty (only stochasticity of the simulations).

Given the numbers of workers in each job role (see I) this means that if the index case is selected at random we expect an R number of $\lesssim 1$ in the parcel work-setting, and ≈ 1 in the large-item setting. Therefore, without any interventions our model predicts that these setting are very likely to see small outbreaks. Given the uncertainty in the underlying parameters, these baseline characteristics need to be considered as a "best guess" case. Bearing this in mind, there remains a great deal to be learned from quantifying the relative impact of various non-pharmaceutical interventions.

The average number of secondary cases in each job role and via each contact route is summarised for each workplace in figures 13 and 14.

a. Parcel delivery: Role of cohort size and mixing

Figure 9 shows the effect of increasing the number of work cohorts (and thereby reducing cohort size) in the parcel delivery work setting, as well as changing the rate at which staff switch between cohorts. Cohort-size only makes the large difference in the case where the index case is a member of office staff. This is because separating into different offices reduces aerosol transmission. In the case of driver/picker cohorts, the underlying model assumptions mean that increasing the cohort size does not change the total amount of contact time (it is simply spread over more contacts). Therefore cohort size only makes a difference to outbreak

probability when there is significant enough transmission via this route that saturation effects can occur. In our model this is the case for picker staff, where the effect is small, but not drivers.

Similarly, figure 9 also shows that increasing the rate at which employees move between cohorts (f_c) has very little effect on outbreak probability. Drivers are predicted to be much less likely to cause an outbreak due to their reduced time spent in the workplace.

Thus we predict that, for these settings, cohort size effects are most important when considering shared indoor spaces such as offices. In well ventilated spaces, where workers are generally spread out and only make contact intermittently, the dominant factor to consider is the total F2F contact time that each employee has with colleagues (not the number of distinct contacts). Note this ceases to be true for longer interactions where transmission risk is higher, as will be demonstrated in the following section.

FIG. 9. Estimated probability of outbreak (defined as more than 3 secondary cases) resulting from a single index case plotted against the cohort flux f_c in days^{-1}. Each marker shows the mean of 10,000 simulations, with shaded error region estimated using a bootstrapping process [52]. Point-source outbreaks where the source case was (a) a driver, (b) a picker; (c) an office worker. Each line in each figure compares simulations with different numbers of teams used for that job role, shown as the number of workers per team on average. In each figure, the job roles not shown have the default team size and $p_{\text{isol}} = 0.9$ is assumed.

b. Large-item delivery: Role of pair work and longer customer exposure

We now consider the case of workplaces that deliver large-items (e.g. furniture, white goods, etc.), such that drivers and pickers work in pairs to perform their tasks. This means they are in close-contact with one another for long periods of the day, increasing the risk of

transmission. In figure 10 we consider 4 intervention scenarios:

1. No intervention: pairings are picked randomly at the start of each shift.

2. Fixed pairings: pairs are fixed and isolation of one partner automatically triggers isolation of the other.

3. Windows open: transmission rate between drivers sharing a cabin assumed to be the same as outside transmission rates, rather than inside.

4. Combination of scenarios 2 + 3.

Figure 10(a) shows the sizeable impact that the fixed pairings intervention has on the baseline dynamics. In particular, when the index case is a driver, the baseline dynamics are dominated by pair transmission (as shown in supplementary figure 14), and more-so for driver pairs due to the time spent in a shared cabin, which we assume to be higher risk than close-contact transmission in better-ventilated settings, such as the warehouse or on the doorstep. The randomly switching pairs mean that all drivers are connected by this transmission route, resulting in a larger number of secondary cases. Fixed pairings (scenario 2) close off these chains, meaning drivers can infect at most one person via this route, and that person then cannot infect anybody else via this route.

On the other hand, when the index case is a warehouse worker, or when we assume "open windows" for drivers, figure 10(a) shows that changing from random to fixed pairings does not have a large effect on transmission. This indicates that, daily contact within picker-pairs (or driver-pairs with open windows) are not predicted to be so high-risk to see a saturation effect. Note that this result is sensitive to the underlying parameterisation, and so has significant uncertainty associated with it.

Figure 10(b) compares the risk to customers related to a point-source outbreak with a driver index case in the large-item delivery workplace vs. the parcel workplace. It is clear that, for each individual customer there is increased risk (due to the longer contact time, chance of home entry needed). Nonetheless, the total number of customers likely to be infected is comparable in the two cases, owing to the large number of deliveries carried out by each driver in the parcel delivery setting. In both cases, even without interventions, this probability is predicted to be small (0.18 ± 0.005 and 0.35 ± 0.008 customers infected per simulation in the parcel and large-item settings respectively). However, in the event of a successful workplace outbreak (i.e. more than 5% of the workforce infected), this increases

to 0.90 ± 0.10 and 1.01 ± 0.02 customer infections for the parcel and large-item delivery workplaces respectively.

We conclude that pair-work can pose a high-risk of transmission in these settings, in which case fixed pairings in combination with pair isolation is an effective measure to break transmission chains and reduce the probability of a workplace outbreak. Generally, we predict that home delivery is unlikely to seed a significant number of new infections in the community, except in cases where there is a workplace outbreak. Thus, extra measures to protect customers (contactless delivery, mask wearing indoors etc.) will have likely made a meaningful impact when prevalence in the workplace was high.

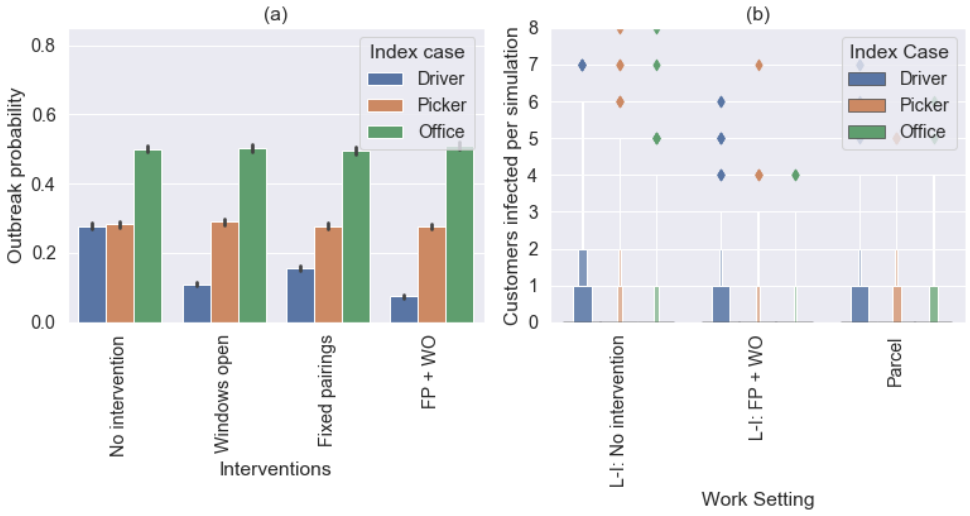

FIG. 10. (a) Simulated probability of a outbreak (defined as more than 2 secondary cases) in a large-item delivery workplace where close-contact pair work is required by driver and picker staff. Four scenarios are shown: no intervention (staff are randomly paired each day); driver pairs travel with window open (transmission rate constant reduced to 1/5 of original value in this setting); fixed pairs (people always work with the same partner); and both of these interventions simultaneously (fixed pairs and windows open). Each bar represents 10,000 simulations, error bars indicate uncertainty in the mean, estimated via a bootstrapping method [52]. (b) Boxen plots of the number of customers infected per point-source outbreak simulation in the large-item (LI) delivery setting with either no or both interventions and the parcel delivery setting with default parameters.

c. Effects of presenteeism

In this model we define presenteeism as working with symptoms of COVID-19 (as we do not model other sickness absences explicitly). On average, 50% of the employees in our simulations develop symptoms relevant for isolation, and if they isolate then they do not attend work for the following 10 days (but household transmission between employees is assumed unaffected). Note that we do not model the effects of illness severity (e.g. prolonged symptoms after recovery, hospital stays, or even death).

Figure 11 shows the effect of increasing self-isolation rates among symptomatic individuals in both work settings, for various values of H, the house-sharing factor. Outbreak probability reduces linearly with isolation adherence, and the proportional effect is larger when house-sharing is rare.

Figure 12 shows the impact of p_{isol} in the large-item delivery setting. The impacts are similar in this workplace to the parcel setting. Comparing the impact with and without fixed-pair isolation policies shows that this interventions results in a slightly larger relative reduction in outbreak probability as presenteeism is reduced. This shows that the combination of this policy with efforts to reduce presenteeism has a larger combined effect than either measure independently, but only in the case of driver index cases. However, we do not see any impact when the index case is a picker or an office staff member, reflecting that the transmission dynamics in these groups are somewhat indepedent of the drivers in our model.

To conclude, adherence to isolation measures are predicted to make a substantial difference to transmission dynamics, particularly in the case where close-contact pairs are both isolated when one develops symptoms. We saw a less-strong effect for household isolation in our model even when a large fraction of workers share accommodation, this is because we assumed that this measure does not prevent household transmission, which was the dominant transmission mode in this scenario. This stresses the importance of messaging around measures to reduce within-household transmission as well isolation measures.

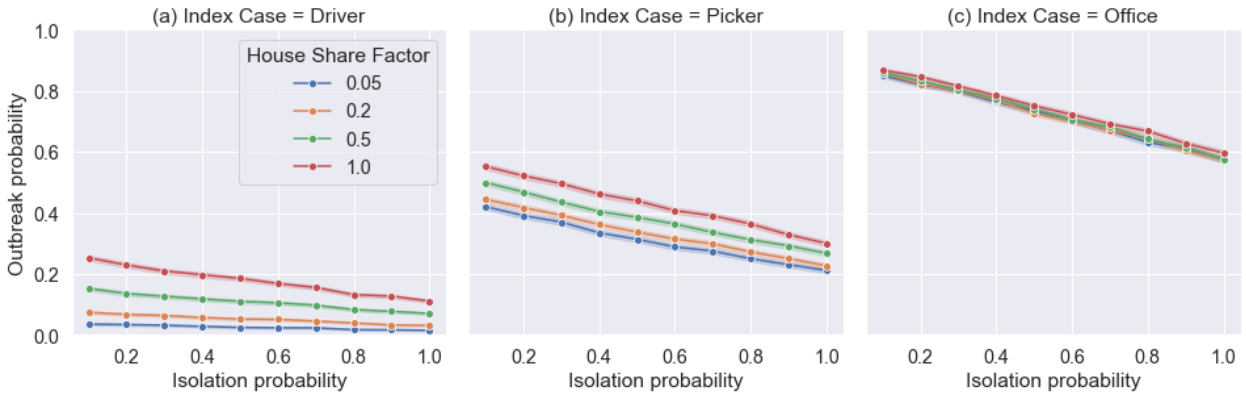

FIG. 11. Dependence of simulated outbreak probability on the self-isolation adherence probability p_{isol} in the model parcel delivery workplace. The different curves show the effect of increasing the house-sharing factor H as labelled.

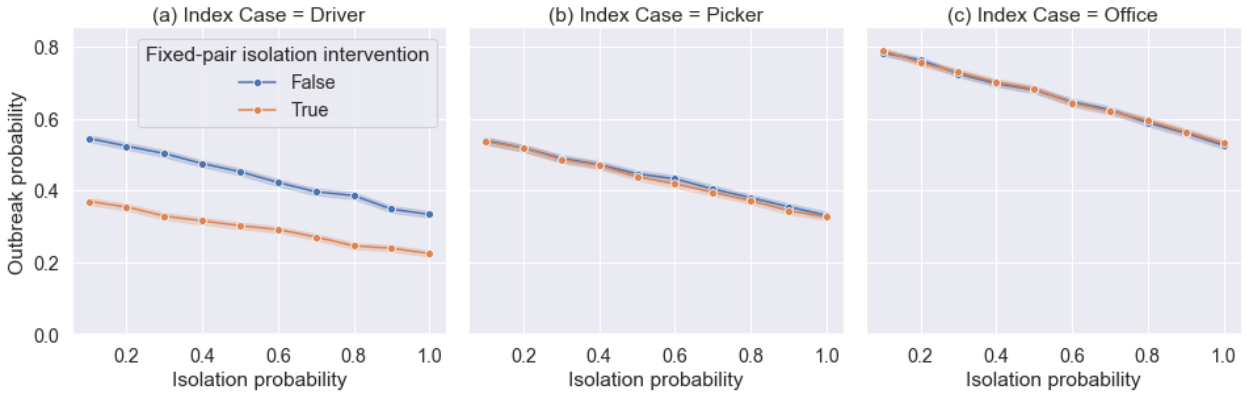

FIG. 12. Dependence of simulated outbreak probability on the self-isolation adherence probability p_{isol} in the model large-item delivery setting. The different curves show the effect of adding a fixed-pairs isolation intervention, as described in the previous section.

Appendix D: Sensitivity to assumptions and parameter choices

1. Baseline transmission rates by job role and contact type

The average number of secondary cases from a points source outbreak (using the baseline parameters used in section C) is broken down by job role of the index case, the secondary case and the contact route for each work setting in figures 13 and 14.

FIG. 13. Stacked bar charts of the mean number of simulated secondary infections resulting from a single index case in (a) a driver, (b) a picker, or (c) an office worker. Each bar shows secondary infections in each group of staff broken down by transmission route, as recorded in table II. Note that the "shared spaces" contacts does not include contacts from sharing an office, these are counted as "cohort" interactions for office staff.

FIG. 14. Stacked bar charts of the mean number of simulated secondary infections resulting from a single index case in (a) a driver, (b) a picker, or (c) an office worker. Each bar shows secondary infections in each group of staff broken down by transmission route. Labels have the same meaning as in figure 13 with the addition of 'pair' indicating infections due to pair work.

2. Transmission parameters

The baseline transmission rate for F2F contacts is derived from multiple sources, but these are largely observational studies and involve a number of assumptions. It is therefore useful to observe how some of the key results are affected if the transmission rate is higher (e.g.

due to more transmissible variants, or due to error in the transmission rate used). Figure 15 shows how the histogram of secondary case numbers changes as the transmission rate β_{F2F} is increased (note we assume that shared-space transmission also increases proportionally). Assuming a random index case, we see a transition from an exponential-type distribution to a multi-modal distribution, as the workplace R-number exceeds 1 and most introductions result in several secondary cases. In these cases, NPIs can have a much more significant impact, as they can push the workplace R-value back to below 1.

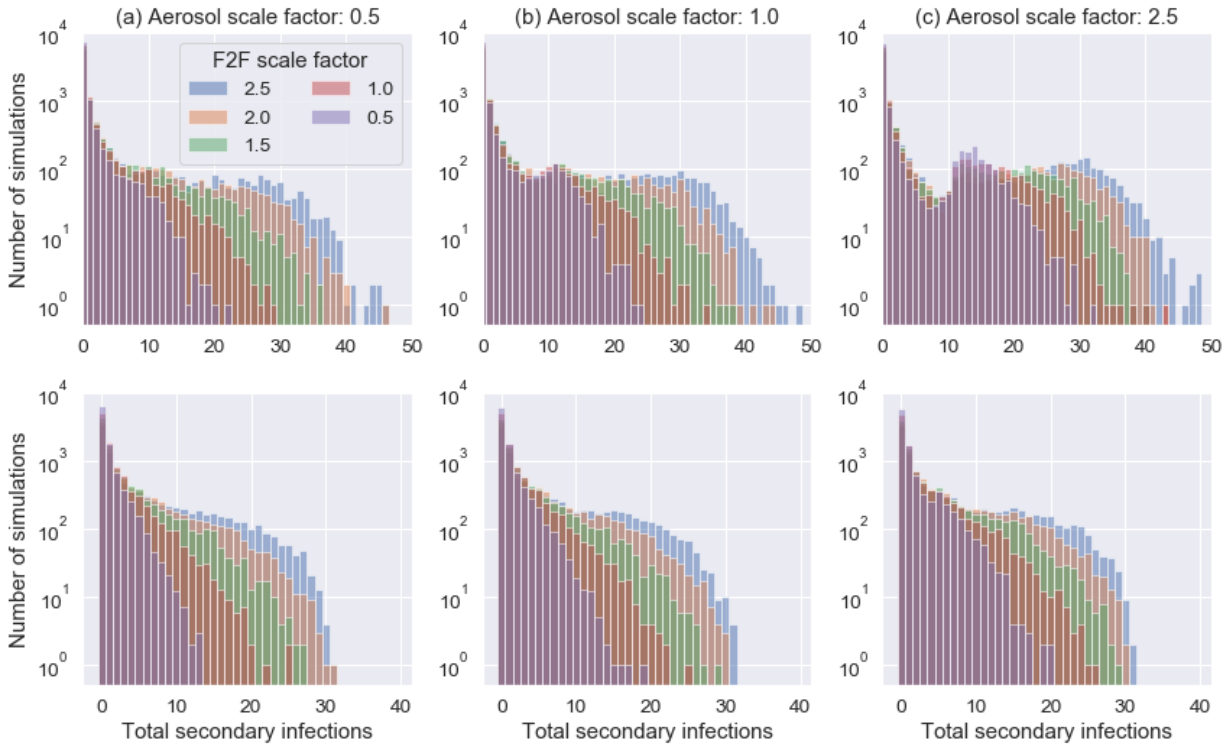

FIG. 15. Histograms of secondary cases resulting from a single index case in the two workplace types simulated for different rates of F2F and aerosol transmission. The top row shows the parcel work setting, while the bottom row is the large-item setting. For each set of simulations, the transmission rate for F2F contacts is multiplied by "F2F scale factor", and the transmission rate for aerosol contacts is multiplied by "Aerosol scale factor". Note that for the large-item workplace we assume that the fixed-pair isolation intervention is applied and in both cases $p_{\text{isol}} = 0.9$. We also assume that the index case is selected randomly.

Second, the fomite transmission parameter is an unknown in the model, so it is important to see for what values it must take for fomite transmission to be significant. In figure 16

we see that increasing the fomite transmission by a factor of 10 makes a relatively minor difference to the outcome of point-source outbreaks originating with a picker (it has a much smaller effect for other index cases). However, the change is substantial when increasing by another factor of 10, suggesting that, if this were the case, it would be a dominant mode of transmission and a significant contributor to overall workplace transmission. Note that, even though the effect is much less significant in the large-items workplace, the β_{FOM} value might actually be larger in this environment, since these items require more force to move (which can affect surface deposition rates) and may require more overall close-contact with the item.

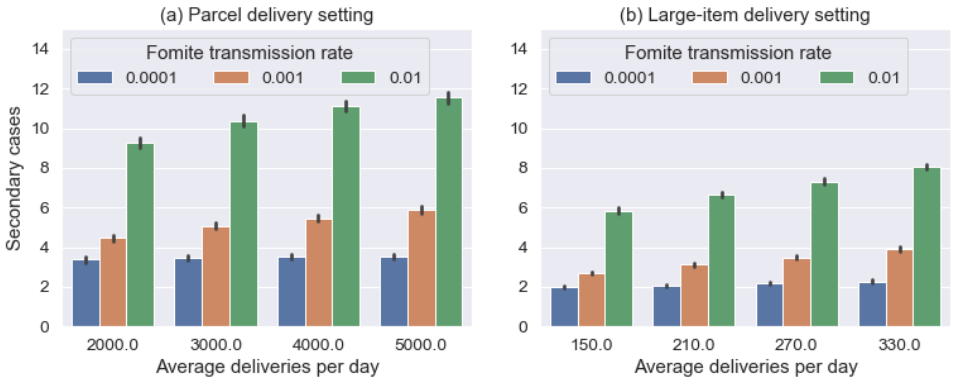

FIG. 16. The mean number of secondary cases resulting from a single index case in the two workplace types plotted for 3 values of β_{FOM} at varying levels of demand for deliveries (x-axis). Note that for the large-item workplace we assume that the fixed-pair isolation intervention is applied and in both cases $p_{\text{isol}} = 0.9$.

3. Number of employees

The influence of overall workplace size is largely controlled by how we assume the contact networks scale in warehouses with fewer/more staff. In order to test this we use simulate workplace sizes corresponding to the upper and lower quartiles of the datasets in section A 1. We scale the workplace size by factor $0.5 \leq r \leq 2$ in the parcel setting and $0.5 \leq r \leq 3$ in the pairs setting. We assume that the parameters scale as follow

$$\{N_D, N_L, N_O\} \to \{\lfloor rN_D \rceil, \lfloor rN_L \rceil, \lfloor rN_O \rceil\} \tag{D1}$$

$$\{T_D, T_L, T_O\} \to \{\lfloor rT_D \rceil, \lfloor rT_L \rceil, \lfloor rT_O \rceil\} \tag{D2}$$

while the definition of p_c remains the same (and so decreases with workplace size).

Figure 17 shows the results of point-source outbreak simulations in the two settings across the range of feasible workplace size scalings. We see that the number of secondary cases resulting from the outbreak is increases with workplace size, although this is mostly explained by the increase in office cohort size (the sharp reduction occurs when the number of teams is increased). This is because, for the parameters used here, most outbreaks become extinct. Therefore this means that the outbreak probability, as defined here, actually drops as workplace size increases, but this is an artifact of choosing 5% as the threshold for an outbreak.

FIG. 17. The mean number of secondary cases resulting from a point-source outbreak in the two workplace types plotted against workplace scale factor. Note that for the large-item workplace we assume that the fixed-pair isolation intervention is applied and in both cases $p_{\text{isol}} = 0.9$. We assume the index case is selected at random.

It is worth noting though that, with greater mixing rates than simulated here, larger workplaces could pose a larger risk of outbreak because of the presence of a larger susceptible population.

4. Mixing rates

We vary the amount of mixing in the workplace by changing the parameter p_c. As p_c increases, not only do more contacts occur but also contacts between different job roles become more frequent. The parameter ρ_D remains fixed at 0.1, so drivers still have less

contact than the other job roles. Figure 18 shows how the number of secondary cases in a point-source outbreak increases as p_c is increased for each workplace.

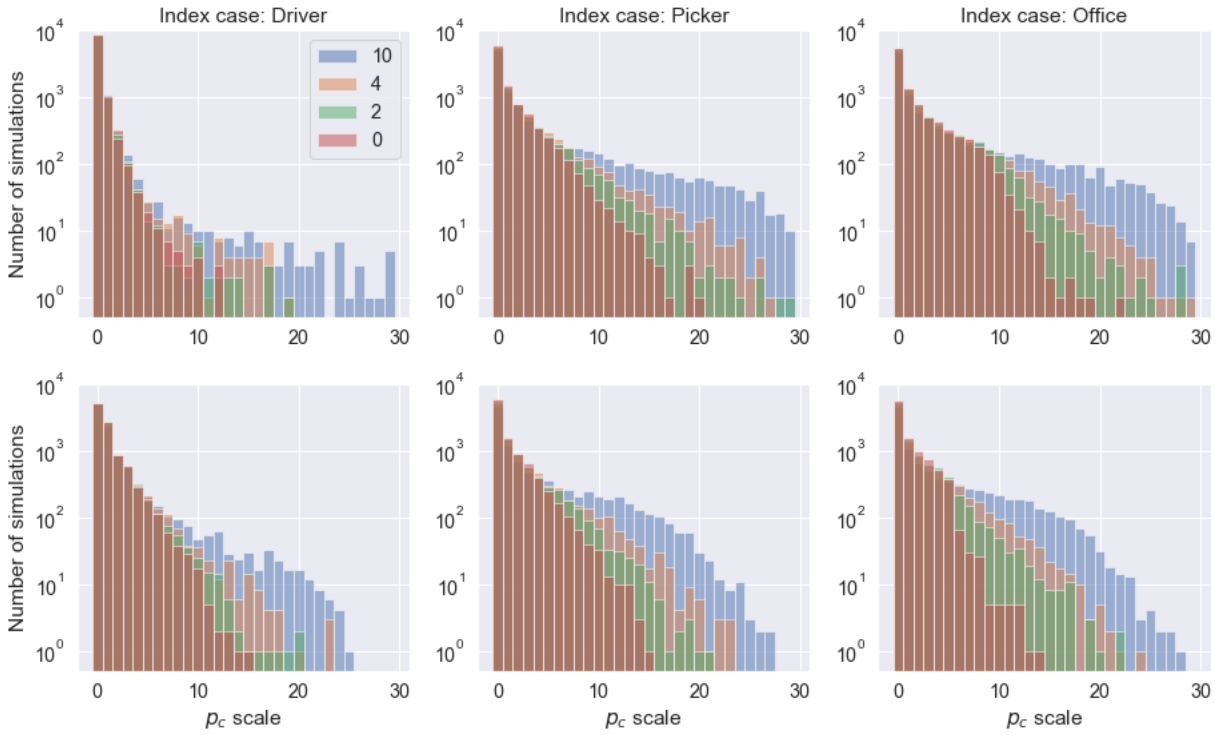

FIG. 18. Histograms of the number of secondary cases resulting from a single index case in the two workplace types plotted for different scalings of $p_c(N_D + N_L + N_O)$. The top row shows the parcel delivery setting, while the bottom row is large-item setting, and each column is for the index-case labelled. Note that for the large-item workplace we assume that the fixed-pair isolation intervention is applied and in both cases $p_{\text{isol}} = 0.9$. Note also the logarithmic scale.

[1] Apex Insight. UK Parcels Market Insight Report. Technical report, 2020. URL `UKParcelsMarketInsightReport2020`.

[2] Hua Wei, Sarah Daniels, Carl A. Whitfield, Yang Han, David W. Denning, Ian Hall, Martyn Regan, Arpana Verma, and Martie van Tongeren. Agility and sustainability: A qualitative evaluation of COVID-19 Non-pharmaceutical Interventions (NPIs) in the UK logistics sector.

Technical report, medRxiv, January 2022. URL https://www.medrxiv.org/content/10.1101/2022.01.28.22270013v1. Type: article.

[3] Koen B. Pouwels, Thomas House, Julie V. Robotham, Paul J. Birrell, Andrew B. Gelman, Nikola Bowers, Ian Boreham, Heledd Thomas, James Lewis, Iain Bell, John I. Bell, John N. Newton, Jeremy Farrar, Ian Diamond, Pete Benton, Ann Sarah Walker, Joshua Abramsky, Daniel Ayoubkhani, Heather Bovill, Dominic Brown, Garnett Compton, James Cooper, Emily Connors, Katie Davies, Claire Dawson, Max Engledew, Onyinye Ezeya, Narcisa Florea, David Foster, Leah Harris, Phillippa Haughton, Nigel Henretty, Tony Hitching, Sarah Henry, Lee Hood, Gareth James, Jaya Jassi, Joe Jenkins, Katherine Kent, Alex Lambert, Maria Ledgeway, Charles Lound, Victoria Masding, Salah Merad, Tibor Mezzei, David Morrissey, Lisa Moore, Ian O'Sullivan, Ellie Osborn, Vasita Patel, Piotr Pawelek, Tristan Pett, Melissa Randall, Craig Smith, Peter Stokes, Eliza Swinn, Esther Sutherland, Tina Thomas, Maggie Vidler, Alison Wiles, Craig Williams, Nick Woodhill, Helena Jordan, Tim Sheppard, Leontia Gribben, Dan Moody, and Leigh Curry. Community prevalence of SARS-CoV-2 in England: Results from the ONS coronavirus infection survey pilot. *medRxiv*, (165):1–13, 2020. doi: 10.1101/2020.07.06.20147348.

[4] Zachary J. Madewell, Yang Yang, Ira M. Longini, M. Elizabeth Halloran, and Natalie E. Dean. Household transmission of SARS-CoV-2: A systematic review and meta-analysis of secondary attack rate. *medRxiv*, 42(4):1, 2020. ISSN 1098-6596. doi:10.1101/2020.07.29.20164590. ISBN: 9788578110796 _eprint: arXiv:1011.1669v3.

[5] Esteban Ortiz-Prado, Aquiles R. Henriquez-Trujillo, Ismar A. Rivera-Olivero, Tannya Lozada, and Miguel Angel Garcia-Bereguiain. High prevalence of SARS-CoV-2 infection among food delivery riders. A case study from Quito, Ecuador. *Sci. Total Environ.*, 770, 2021. ISSN 18791026. doi:10.1016/j.scitotenv.2021.145225. Publisher: Elsevier B.V.

[6] Trystan Leng, Edward M Hill, Robin N Thompson, Michael J Tildesley, Matt J Keeling, and Louise Dyson. Assessing the impact of secondary school reopening strategies on within-school COVID-19 transmission and absences: a modelling study. *medRxiv*, page 2021.02.11.21251587, 2021. doi:10.1101/2021.02.11.21251587. URL https://doi.org/10.1101/2021.02.11.21251587.

[7] Giovanni S.P. Malloy, Lisa Puglisi, Margaret L. Brandeau, Tyler D. Harvey, and Emily A. Wang. Effectiveness of interventions to reduce COVID-19 transmission in a large urban jail: A model-based analysis. *BMJ Open*, 11(2), 2021. ISSN 20446055. doi:10.1136/bmjopen-2020-042898.

[8] Cliff C. Kerr, Robyn M. Stuart, Dina Mistry, Romesh G. Abeysuriya, Katherine Rosenfeld, Gregory R. Hart, Rafael C. Núñez, Jamie A. Cohen, Prashanth Selvaraj, Brittany Hagedorn, Lauren George, Michał Jastrzebski, Amanda S. Izzo, Greer Fowler, Anna Palmer, Dominic Delport, Nick Scott, Sherrie L. Kelly, Caroline S. Bennette, Bradley G. Wagner, Stewart T. Chang, Assaf P. Oron, Edward A. Wenger, Jasmina Panovska-Griffiths, Michael Famulare, and Daniel J. Klein. Covasim: An agent-based model of COVID-19 dynamics and interventions. *PLOS Computational Biology*, 17(7):e1009149, July 2021. ISSN 1553-7358. doi: 10.1371/journal.pcbi.1009149. URL `https://journals.plos.org/ploscompbiol/article?id=10.1371/journal.pcbi.1009149`. Publisher: Public Library of Science.

[9] Edward M. Hill, Benjamin D. Atkins, Matt J. Keeling, Louise Dyson, and Michael J. Tildesley. A network modelling approach to assess non-pharmaceutical disease controls in a worker population: An application to SARS-CoV-2. *medRxiv*, 2020. doi:10.1101/2020.11.18.20230649.

[10] Edward M. Hill, Benjamin D. Atkins, Matt J. Keeling, Louise Dyson, and Michael J. Tildesley. A network modelling approach to assess non-pharmaceutical disease controls in a worker population: An application to SARS-CoV-2. *PLOS Computational Biology*, 17 (6):e1009058, June 2021. ISSN 1553-7358. doi:10.1371/journal.pcbi.1009058. URL `https://journals.plos.org/ploscompbiol/article?id=10.1371/journal.pcbi.1009058`. Publisher: Public Library of Science.

[11] Martyn Fyles, Elizabeth Fearon, Christopher Overton, null null, Tom Wingfield, Graham F. Medley, Ian Hall, Lorenzo Pellis, and Thomas House. Using a household-structured branching process to analyse contact tracing in the SARS-CoV-2 pandemic. *Philosophical Transactions of the Royal Society B: Biological Sciences*, 376(1829):20200267, July 2021. doi: 10.1098/rstb.2020.0267. URL `https://royalsocietypublishing.org/doi/full/10.1098/rstb.2020.0267`. Publisher: Royal Society.

[12] Jonathan J. Deeks and Angela E. Raffle. Lateral flow tests cannot rule out SARS-CoV-2 infection. *BMJ*, 371(December):1–2, 2020. ISSN 17561833. doi:10.1136/bmj.m4787.

[13] Jacqui Wise. Covid-19: Lateral flow tests miss over half of cases, Liverpool pilot data show. *BMJ*, 371:m4848, 2020. ISSN 17561833. doi:10.1136/bmj.m4848.

[14] Hamish Houston, Ankur Gupta-Wright, Edward Toke-Bjolgerud, James Biggin-Lamming, and Laurence John. Diagnostic accuracy and utility of SARS-CoV-2 antigen lateral flow assays in medical admissions with possible COVID-19. *J. Hosp. Infect.*, (xxxx):18–20, 2021. ISSN 01956701. doi:10.1016/j.jhin.2021.01.018.

[15] Jack Ferguson, Steven Dunn, Angus Best, Jeremy Mirza, Benita Percival, Megan Mayhew, Oliver Megram, Fiona Ashford, Thomas White, Emma Moles-Garcia, Liam Crawford, Tim Plant, Andrew Bosworth, Michael Kidd, Alex Richter, Jonathan Deeks, and Alan McNally. Validation testing to determine the effectiveness of lateral flow testing for asymptomatic SARS-CoV-2 detection in low prevalence settings. *medRxiv*, (1):1–57, 2020. doi: 10.1101/2020.12.01.20237784.

[16] Achim Wolf, Jack Hulmes, and Susan Hopkins. Lateral flow device specificity in phase 4 (post-marketing) surveillance. Technical report, 2021. URL `https://www.gov.uk/government/publications/lateral-flow-device-specificity-in-phase-4-post-marketing-surveillance`.

[17] Kieran A. Walsh, Karen Jordan, Barbara Clyne, Daniela Rohde, Linda Drummond, Paula Byrne, Susan Ahern, Paul G. Carty, Kirsty K. O'Brien, Eamon O'Murchu, Michelle O'Neill, Susan M. Smith, Máirín Ryan, and Patricia Harrington. SARS-CoV-2 detection, viral load and infectivity over the course of an infection. *J. Infect.*, 81(3):357–371, 2020. ISSN 15322742. doi:10.1016/j.jinf.2020.06.067. URL `https://doi.org/10.1016/j.jinf.2020.06.067`. Publisher: Elsevier Ltd.

[18] Bernard La Scola, Marion Le Bideau, Julien Andreani, Van Thuan Hoang, Clio Grimaldier, Philippe Colson, Philippe Gautret, and Didier Raoult. Viral RNA load as determined by cell culture as a management tool for discharge of SARS-CoV-2 patients from infectious disease wards. *Eur. J. Clin. Microbiol. Infect. Dis.*, 39(6):1059–1061, June 2020. ISSN 0934-9723. doi:10.1007/s10096-020-03913-9. URL `http://link.springer.com/10.1007/s10096-020-03913-9`. ISBN: 1009602003913 Publisher: European Journal of Clinical Microbiology & Infectious Diseases.

[19] Jeroen J.A. van Kampen, David A.M.C. van de Vijver, Pieter L.A. Fraaij, Bart L. Haagmans, Mart M. Lamers, Nisreen Okba, Johannes P.C. van den Akker, Henrik Endeman, Diederik A.M.P.J. Gommers, Jan J. Cornelissen, Rogier A.S. Hoek, Menno M. van der Eerden, Dennis A. Hesselink, Herold J. Metselaar, Annelies Verbon, Jurriaan E.M. de Steenwinkel, Georgina I. Aron, Eric C.M. van Gorp, Sander van Boheemen, Jolanda C. Voermans, Charles A.B. Boucher, Richard Molenkamp, Marion P.G. Koopmans, Corine Geurtsvankessel, and Annemiek A. van der Eijk. Duration and key determinants of infectious virus shedding in hospitalized patients with coronavirus disease-2019 (COVID-19). *Nat. Commun.*, 12(1):8–13, 2021. ISSN 20411723. doi:10.1038/s41467-020-20568-4. Publisher: Springer US.

[20] Tim Peto. COVID-19: Rapid Antigen detection for SARS-CoV-2 by lateral flow assay: a national systematic evaluation for mass-testing. *medRxiv*, page 2021.01.13.21249563, 2021. URL http://medrxiv.org/content/early/2021/01/15/2021.01.13.21249563.abstract.

[21] Sarah Daniels, Hua Wei, Yang Han, Heather Catt, David W. Denning, Ian Hall, Martyn Regan, Arpana Verma, Carl A. Whitfield, and Martie van Tongeren. Risk factors associated with respiratory infectious disease-related presenteeism: a rapid review. Technical report, April 2021. URL https://www.medrxiv.org/content/10.1101/2021.04.12.21255302v1. Company: Cold Spring Harbor Laboratory Press Distributor: Cold Spring Harbor Laboratory Press Label: Cold Spring Harbor Laboratory Press Type: article.

[22] The microCOVID Project. White paper. 2020.

[23] Lennard Y W Lee, Stefan Rozmanowski, Matthew Pang, Andre Charlett, Charlotte Anderson, Gareth J Hughes, Matthew Barnard, Leon Peto, Richard Vipond, Alex Sienkiewicz, John Bell, Derrick W Crook, Nick Gent, A Sarah Walker, David W Eyre, and Tim Ea. An observational study of SARS-CoV-2 infectivity by viral load and demographic factors and the utility lateral flow devices to prevent transmission. 2021.

[24] G. Cortellessa, L. Stabile, F. Arpino, D. E. Faleiros, W. van den Bos, L. Morawska, and G. Buonanno. Close proximity risk assessment for SARS-CoV-2 infection. *Science of The Total Environment*, 794:148749, November 2021. ISSN 0048-9697. doi:10.1016/j.scitotenv.2021.148749. URL https://www.sciencedirect.com/science/article/pii/S0048969721038213.

[25] Neeltje van Doremalen, Trenton Bushmaker, Dylan H. Morris, Myndi G. Holbrook, Amandine Gamble, Brandi N. Williamson, Azaibi Tamin, Jennifer L. Harcourt, Natalie J. Thornburg, Susan I. Gerber, James O. Lloyd-Smith, Emmie de Wit, and Vincent J. Munster. Aerosol and Surface Stability of SARS-CoV-2 as Compared with SARS-CoV-1. *N. Engl. J. Med.*, 382(16):1564–1567, April 2020. ISSN 0028-4793. doi:10.1056/NEJMc2004973. URL http://www.nejm.org/doi/10.1056/NEJMc2004973.

[26] Ruian Ke, Pamela P. Martinez, Rebecca L. Smith, Laura L. Gibson, Agha Mirza, Madison Conte, Nicholas Gallagher, Chun Huai Luo, Junko Jarrett, Abigail Conte, Tongyu Liu, Mireille Farjo, Kimberly K. O. Walden, Gloria Rendon, Christopher J. Fields, Leyi Wang, Richard Fredrickson, Darci C. Edmonson, Melinda E. Baughman, Karen K. Chiu, Hannah Choi, Kevin R. Scardina, Shannon Bradley, Stacy L. Gloss, Crystal Reinhart, Jagadeesh Yedetore, Jessica Quicksall, Alyssa N. Owens, John Broach, Bruce Barton, Peter Lazar, William J. Heetderks, Matthew L. Robinson, Heba H. Mostafa, Yukari C. Manabe, Andrew Pekosz, David D. McManus, and Christopher B. Brooke. Daily sampling of early SARS-

CoV-2 infection reveals substantial heterogeneity in infectiousness. Technical report, July 2021. URL https://www.medrxiv.org/content/10.1101/2021.07.12.21260208v1. Company: Cold Spring Harbor Laboratory Press Distributor: Cold Spring Harbor Laboratory Press Label: Cold Spring Harbor Laboratory Press Type: article.

[27] Social Care Working Group . SCWG Chairs: Summary of role of shielding, 20 December 2021, 2021. URL https://www.gov.uk/government/publications/scwg-chairs-summary-of-role-of-shielding-20-december-2021.

[28] Carl A Whitfield. Model of SARS-CoV-2 viral load dynamics, infectivity profile, and test-positivity., 2022. URL https://github.com/CarlWhitfield/Viral_load_testing_COV19_model.

[29] Carl A Whitfield. Model of SARS-CoV-2 transmission in delivery workplaces, 2022. URL https://github.com/CarlWhitfield/Workplace_delivery_transmission.

[30] Joel Hellewell, Timothy W. Russell, Rupert Beale, Gavin Kelly, Catherine Houlihan, Eleni Nastouli, and Adam J. Kucharski. Estimating the effectiveness of routine asymptomatic PCR testing at different frequencies for the detection of SARS-CoV-2 infections. *medRxiv*, 2020. doi:10.1101/2020.11.24.20229948.

[31] Billy J. Quilty, Samuel Clifford, Joel Hellewell, Timothy W. Russell, Adam J. Kucharski, Stefan Flasche, W. John Edmunds, Katherine E. Atkins, Anna M. Foss, Naomi R. Waterlow, Kaja Abbas, Rachel Lowe, Carl A. B. Pearson, Sebastian Funk, Alicia Rosello, Gwenan M. Knight, Nikos I. Bosse, Simon R. Procter, Georgia R. Gore-Langton, Alicia Showering, James D. Munday, Katharine Sherratt, Thibaut Jombart, Emily S. Nightingale, Yang Liu, Christopher I. Jarvis, Graham Medley, Oliver Brady, Hamish P. Gibbs, David Simons, Jack Williams, Damien C. Tully, Stefan Flasche, Sophie R. Meakin, Kevin Zandvoort, Fiona Y. Sun, Mark Jit, Petra Klepac, Matthew Quaife, Rosalind M. Eggo, Frank G. Sandmann, Akira Endo, Kiesha Prem, Sam Abbott, Rosanna Barnard, Yung-Wai D. Chan, Megan Auzenbergs, Amy Gimma, C. Julian Villabona-Arenas, and Nicholas G. Davies. Quarantine and testing strategies in contact tracing for SARS-CoV-2: a modelling study. *The Lancet Public Health*, 6(3):e175–e183, March 2021. ISSN 2468-2667. doi:10.1016/S2468-2667(20)30308-X. URL https://www.thelancet.com/journals/lanpub/article/PIIS2468-2667(20)30308-X/abstract. Publisher: Elsevier.

[32] Kaitlin Piper, Ada Youk, A. Everette James Iii, and Supriya Kumar. Paid sick days and stay-at-home behavior for influenza. *PLOS ONE*, 12(2):e0170698, February 2017. ISSN 1932-6203. doi:10.1371/journal.pone.0170698. URL https://journals.plos.org/plosone/

article?id=10.1371/journal.pone.0170698. Publisher: Public Library of Science.

[33] Faruque Ahmed, Sara Kim, Mary Patricia Nowalk, Jennifer P. King, Jeffrey J. VanWormer, Manjusha Gaglani, Richard K. Zimmerman, Todd Bear, Michael L. Jackson, Lisa A. Jackson, Emily Martin, Caroline Cheng, Brendan Flannery, Jessie R. Chung, and Amra Uzicanin. Paid Leave and Access to Telework as Work Attendance Determinants during Acute Respiratory Illness, United States, 2017–2018. *Emerging Infectious Diseases*, 26(1):26–33, January 2020. ISSN 1080-6040. doi:10.3201/eid2601.190743. URL https://www.ncbi.nlm.nih.gov/pmc/articles/PMC6924903/.

[34] Florian Poydenot, Ismael Abdourahamane, Elsa Caplain, Samuel Der, Jacques Haiech, Antoine Jallon, Inés Khoutami, Amir Loucif, Emil Marinov, and Bruno Andreotti. Risk assessment for long and short range airborne transmission of SARS-CoV-2, indoors and outdoors, using carbon dioxide measurements. *medRxiv*, page 2021.05.04.21256352, May 2021. doi: 10.1101/2021.05.04.21256352. URL https://www.medrxiv.org/content/10.1101/2021.05.04.21256352v1. Publisher: Cold Spring Harbor Laboratory Press.

[35] Alexandra LJ Freeman, Simon Parker, Catherine Noakes, Shaun Fitzgerald, Alexandra Smyth, Ron Macbeth, David Spiegelhalter, and Harry Rutter. Expert elicitation on the relative importance of possible SARS-CoV-2 transmission routes and the effectiveness of mitigations. *BMJ Open*, 11(12):e050869, December 2021. ISSN 2044-6055, 2044-6055. doi:10.1136/bmjopen-2021-050869. URL http://bmjopen.bmj.com/content/11/12/e050869. Publisher: British Medical Journal Publishing Group Section: Public health.

[36] Ana K. Pitol and Timothy R. Julian. Community Transmission of SARS-CoV-2 by Surfaces: Risks and Risk Reduction Strategies. *Environmental Science & Technology Letters*, 8(3):263–269, March 2021. doi:10.1021/acs.estlett.0c00966. URL https://doi.org/10.1021/acs.estlett.0c00966. Publisher: American Chemical Society.

[37] Henry C. Burridge, Shiwei Fan, Roderic L. Jones, Catherine J. Noakes, and P. F. Linden. Predictive and retrospective modelling of airborne infection risk using monitored carbon dioxide. *arXiv:2009.02999 [physics]*, February 2021. URL http://arxiv.org/abs/2009.02999. arXiv: 2009.02999.

[38] G. Buonanno, A. Robotto, E. Brizio, L. Morawska, A. Civra, F. Corino, D. Lembo, G. Ficco, and L. Stabile. Link between SARS-CoV-2 emissions and airborne concentrations: closing the gap in understanding. *arXiv:2110.02706 [physics]*, October 2021. URL http://arxiv.org/abs/2110.02706. arXiv: 2110.02706.

[39] Shelly L. Miller, William W Nazaroff, Jose L. Jimenez, Atze Boerstra, Giorgio Buonanno, Stephanie J. Dancer, Jarek Kurnitski, Linsey C. Marr, Lidia Morawska, and Catherine Noakes. Transmission of SARS-CoV-2 by inhalation of respiratory aerosol in the Skagit Valley Chorale superspreading event. *Indoor Air*, 31(2):314–323, 2021. ISSN 1600-0668. doi: 10.1111/ina.12751. URL http://onlinelibrary.wiley.com/doi/abs/10.1111/ina.12751. _eprint: https://onlinelibrary.wiley.com/doi/pdf/10.1111/ina.12751.

[40] Parham Azimi, Zahra Keshavarz, Jose Guillermo Cedeno Laurent, Brent Stephens, and Joseph G. Allen. Mechanistic transmission modeling of COVID-19 on the Diamond Princess cruise ship demonstrates the importance of aerosol transmission. *Proceedings of the National Academy of Sciences*, 118(8), February 2021. ISSN 0027-8424, 1091-6490. doi: 10.1073/pnas.2015482118. URL https://www.pnas.org/content/118/8/e2015482118. Publisher: National Academy of Sciences Section: Physical Sciences.

[41] Lidia Morawska, Julian W. Tang, William Bahnfleth, Philomena M. Bluyssen, Atze Boerstra, Giorgio Buonanno, Junji Cao, Stephanie Dancer, Andres Floto, Francesco Franchimon, Charles Haworth, Jaap Hogeling, Christina Isaxon, Jose L. Jimenez, Jarek Kurnitski, Yuguo Li, Marcel Loomans, Guy Marks, Linsey C. Marr, Livio Mazzarella, Arsen Krikor Melikov, Shelly Miller, Donald K. Milton, William Nazaroff, Peter V. Nielsen, Catherine Noakes, Jordan Peccia, Xavier Querol, Chandra Sekhar, Olli Seppänen, Shin-ichi Tanabe, Raymond Tellier, Kwok Wai Tham, Pawel Wargocki, Aneta Wierzbicka, and Maosheng Yao. How can airborne transmission of COVID-19 indoors be minimised? *Environment International*, 142:105832, September 2020. ISSN 0160-4120. doi:10.1016/j.envint.2020.105832. URL https://www.sciencedirect.com/science/article/pii/S0160412020317876.

[42] Amy E. Benefield, Laura A. Skrip, Andrea Clement, Rachel A. Althouse, Stewart Chang, and Benjamin Muir Althouse. SARS-CoV-2 viral load peaks prior to symptom onset: A systematic review and individual-pooled analysis of coronavirus viral load from 66 studies. *medRxiv*, (425), 2020. doi:10.1101/2020.09.28.20202028.

[43] Michael Marks, Pere Millat-Martinez, Dan Ouchi, Chrissy h Roberts, Andrea Alemany, Marc Corbacho-Monné, Maria Ubals, Aurelio Tobias, Cristian Tebé, Ester Ballana, Quique Bassat, Bàrbara Baro, Martí Vall-Mayans, Camila G-Beiras, Nuria Prat, Jordi Ara, Bonaventura Clotet, and Oriol Mitjà. Transmission of COVID-19 in 282 clusters in Catalonia, Spain: a cohort study. *Lancet Infect. Dis.*, 3099(20):1–8, February 2021. ISSN 14733099. doi: 10.1016/S1473-3099(20)30985-3. URL https://linkinghub.elsevier.com/retrieve/pii/S1473309920309853.

[44] Luca Ferretti, Chris Wymant, Anel Nurtay, Lele Zhao, Robert Hinch, David Bonsall, Michelle Kendall, Joanna Masel, John Bell, Susan Hopkins, A. Marm Kilpatrick, Tim Peto, Lucie Abeler-Dörner, and Christophe Fraser. Modelling the effectiveness and social costs of daily lateral flow antigen tests versus quarantine in preventing onward transmission of COVID-19 from traced contacts. Technical report, August 2021. URL `https://www.medrxiv.org/content/10.1101/2021.08.06.21261725v1`. Company: Cold Spring Harbor Laboratory Press Distributor: Cold Spring Harbor Laboratory Press ISSN: 2126-1725 Label: Cold Spring Harbor Laboratory Press Type: article.

[45] Elizabeth Smith, Wei Zhen, Ryhana Manji, Deborah Schron, Scott Duong, and Gregory J Berry. Analytical and Clinical Comparison of Three Nucleic Acid Amplification Tests for SARS-CoV-2 Detection. *Journal of Clinical Microbiology*, 58(9):8, 2020.

[46] NHS Test and Trace. Dual-technology TESTING ANALYSIS High-Risk Settings. Technical report, November 2021.

[47] Christopher E. Overton, Helena B. Stage, Shazaad Ahmad, Jacob Curran-Sebastian, Paul Dark, Rajenki Das, Elizabeth Fearon, Timothy Felton, Martyn Fyles, Nick Gent, Ian Hall, Thomas House, Hugo Lewkowicz, Xiaoxi Pang, Lorenzo Pellis, Robert Sawko, Andrew Ustianowski, Bindu Vekaria, and Luke Webb. Using statistics and mathematical modelling to understand infectious disease outbreaks: COVID-19 as an example. *ArXiv*, May 2020. URL `http://arxiv.org/abs/2005.04937`. _eprint: 2005.04937.

[48] Kanika Kuwelker, Fan Zhou, Bjørn Blomberg, Sarah Lartey, Karl Albert Brokstad, Mai Chi Trieu, Anders Madsen, Florian Krammer, Kristin G.I. Mohn, Camilla Tøndel, Dagrunn Waag Linchausen, Rebecca J. Cox, and Nina Langeland. High attack rates of SARS-CoV-2 infection through household-transmission: A prospective study. *medRxiv*, 2020. doi: 10.1101/2020.11.02.20224485.

[49] Qin Long Jing, Ming Jin Liu, Zhou Bin Zhang, Li Qun Fang, Jun Yuan, An Ran Zhang, Natalie E. Dean, Lei Luo, Meng Meng Ma, Ira Longini, Eben Kenah, Ying Lu, Yu Ma, Neda Jalali, Zhi Cong Yang, and Yang Yang. Household secondary attack rate of COVID-19 and associated determinants in Guangzhou, China: a retrospective cohort study. *Lancet Infect. Dis.*, 20(10):1141–1150, 2020. ISSN 14744457. doi:10.1016/S1473-3099(20)30471-0.

[50] Toru Watanabe, Timothy A. Bartrand, Mark H. Weir, Tatsuo Omura, and Charles N. Haas. Development of a dose-response model for SARS coronavirus. *Risk Anal.*, 30(7):1129–1138, 2010. ISSN 02724332. doi:10.1111/j.1539-6924.2010.01427.x.

[51] Xiaole Zhang and Jing Wang. Dose-response Relation Deduced for Coronaviruses from COVID-19, SARS and MERS Meta-analysis Results and its Application for Infection Risk Assessment of Aerosol Transmission. *Clin. Infect. Dis.*, 2020. ISSN 1058-4838. doi: 10.1093/cid/ciaa1675.

[52] Michael L Waskom. seaborn: statistical data visualization. *J. Open Source Softw.*, 6(60):3021, 2021. doi:10.21105/joss.03021. URL `https://doi.org/10.21105/joss.03021`. Publisher: The Open Journal.

TABLE II. Summary of the contact routes simulated and the associated transmission rate modifier, duration of contact, and contact distance. These are the values used in all simulations in the main text unless explicitly stated otherwise.

Contact-type	Description	Transmission modifier (c_i)	Duration (τ_i)	Distance
Cohort	F2F contacts that occur within a team or cohort (see section A 4 a for more information).	1 (either indoor or "loud-talking" outdoors)	Drivers: $\tau_{\text{coh}} = 0.25$h Pickers/Office: $\tau_{\text{coh}} = 1$h	1m
Random	F2F contacts that occur randomly in the workplace with weighted probability towards contacts between same job roles (see section A 4 a for more information).	1	$\tau_{\text{rand}} = 10$ min	1m
Large-item handling	Time spent lifting and moving packages in pairs (see section A 4 a for more information).	0.04 (outdoor, no talking)	$\tau_{\text{han}} = 5$ min per delivery	1m
Pair delivery	Contact via sharing a cabin while delivering large-items (see section A 4 a for more information).	0.2 (window closed) 0.04 (window open)	$\tau_{\text{cab}} = 5$ min per delivery	1m
Pair dropoff	Contact between driver pairs during dropping large-item off at customer's property (see section A 4 a for more information).	1.0	$\tau_{\text{drop}} = 3$ min per delivery	1m
Customer	Contact between driver(s) and customer during item delivery	Parcel: 0.2 (outside) Large-item: 1.0, 0.2 (random, 50% inside)	Parcel: 30s per delivery Large-item: 5min per delivery	Parcel: 1m Large-item: 2m
Room-share	Aerosol-mediated contact in poorly ventilated rooms	0.2 (no talking)	$\tau_{\text{off}} = 6$h $\tau_{\text{lun}} = 1$h	6m (see Appendix A)
Car-share	Contact via carpooling to and from work.	1	0.5h	1m
House-	Contact via shared			

Parameter	Description	Value	Source
$\boldsymbol{\mu}_{VL}$	Vector of log-means of [V_p, τ_p, $1/d$, $1/r$].	[17.55, 1.39, -1.20, -0.67]	Fitted to [26]
Σ_{VL}	Log-covariance matrix of [V_p, τ_p, $1/d$, $1/r$].	$\begin{pmatrix} 0.909 & 0.044 & -0.011 & 0.081 \\ 0.044 & 0.033 & 0.029 & 0.005 \\ -0.011 & 0.029 & 0029 & 0.0004 \\ 0.081 & 0.005 & 0.0004 & 0.027 \end{pmatrix}$	Fitted to [26]
$\boldsymbol{\mu}_J$	Vector of log-means of [J_p, h].	[1.263, -0.108]	Fitted to [26]
Σ_J	Log-covariance matrix of [J_p, h].	$\begin{pmatrix} 0.3387 & 0.0265 \\ 0.0265 & 0.1270 \end{pmatrix}$	Fitted to [26]
K_m	Fixed infectivity scale parameter.	4.0×10^6 copies/ml.	[26]
$P_{\max}$	Maximum test positive probability for PCR.	0.83	[44].
[s_t, $log_{10}(V_0)$]	Parameters of PCR probability logistic function	[4.41, 1.93]	Fitted to [45].
V_{cut}	Viral load corresponding to Ct threshold for PCR test	10 copies/ml	Assumed from [20].
$\theta(V_k)$	Test positive probability for LFD.	$\begin{cases} 0.004 & \text{if } V_k \leq 10^2 \\ 0.025 & \text{if } 10^2 < V_k \leq 10^3 \\ 0.087 & \text{if } 10^3 < V_k \leq 10^4 \\ 0.162 & \text{if } 10^4 < V_k \leq 10^5 \\ 0.414 & \text{if } 10^5 < V_k \leq 10^6 \\ 0.651 & \text{if } 10^6 < V_k \leq 10^7 \\ 0.80 & \text{if } V_k > 10^7 \end{cases}$.	[46]
μ_s, σ_s	Mean and standard deviation of gamma-distributed symptom onset time (prior to truncation).	4.84, 2.6 days	[47]

TABLE III. Viral load, infectivity, and test positive probability parameters used in the simulations.

Parameter	Description	Value	Source
V	Room volume.	150 m^3	Approximated ($\approx 7 \times 7 \times 3$)
$\dot{V}_T$	Tidal breathing rate.	0.7 m^3 h^{-1}	Approximated
f	Air changes per hour.	2 h^{-1}	Assumed (typical unventilated office value)
λ	Decay rate of SARS-CoV-2 in air.	0.76 h^{-1}	[25]
n_0/ID_e	Average number of infectious quanta exhaled per hour for an individual infected with SARS-CoV-2	4.0	[34]

TABLE IV. Parameters used to determine the shared-space transmission parameter x_{ss}.